Ecological Monographs, 83(2), 2013, pp. 155–176

Diel phosphorus variation and the stoichiometry of ecosystem metabolism in a large spring-fed river

Matthew J. Cohen,[1,4] Marie J. Kurz,[2] James B. Heffernan,[3] Jonathan B. Martin,[2] Rachel L. Douglass,[1] Chad R. Foster,[1] and Ray G. Thomas[2]

[1]*School of Forest Resources and Conservation, University of Florida, 328 Newins Ziegler Hall, Gainesville, Florida 32611-0410 USA*
[2]*Geological Sciences, University of Florida, 241 Williamson Hall, Gainesville, Florida 32611-2120 USA*
[3]*Nicholas School of the Environment, Duke University, 309A LSRC, Durham, North Carolina 27708-0328 USA*

Abstract. Elemental cycles are coupled directly and indirectly to ecosystem metabolism at multiple time scales. Understanding coupling in lotic ecosystems has recently advanced through simultaneous high-frequency measurements of multiple solutes. Using hourly in situ measurements of soluble reactive phosphorus (SRP), specific conductance (SpC), and dissolved oxygen (DO), we estimated phosphorus (P) retention pathways and dynamics in a large (discharge, $Q \approx 7.5$ m^3/s) spring-fed river (Ichetucknee River, Florida, USA). Across eight multi-day deployments, highly regular diel SRP variation of 3–9 μg P/L (mean ~50 μg P/L) was strongly correlated with DO variation, suggesting photosynthetic control directly via assimilation, and/or indirectly via geochemical reactions. Consistent afternoon SRP maxima and midnight minima suggest peak removal lags gross primary production (GPP) by ~8 hours. Two overlapping processes were evident, one dominant with maximum removal near midnight, the other smaller with maximum removal near midday. Hourly [Ca] measurements during three 24-hour deployments showed consistent afternoon minima, suggesting that calcite precipitates as GPP increases pH and mineral saturation state. Resulting P co-precipitation was modeled using SpC as a [Ca] proxy, yielding a diel P signal adjusted for the primary geochemical retention pathway. P assimilation, the dominant diel signal, was computed by interpolating between daily concentration maxima, both with and without geochemical adjustment, and converting concentration deficits to fluxes using discharge and benthic area. Adjusting for calcite co-precipitation yielded assimilation rates (13.7 ± 5.8 mg $P \cdot m^{-2} \cdot d^{-1}$) strongly correlated with GPP, accounting for 72% ± 9% of gross removal, and ecosystem C:P stoichiometry (466 [± 12]:1) consistent with dominant vascular autotrophs (478 [± 24]:1). Without adjusting for co-precipitation, covariance with GPP was weaker, and C:P implausibly high. Consistent downstream P accumulation, likely from P-rich porewater seepage, varied across deployments (3–22% of total flux) and co-varied with discharge and respiration. Asynchronous N and P assimilation may arise from differential timing of protein and ribosome production, with the latter requiring maximal carbohydrate stores and minimal photolytic interference. This study demonstrates direct and indirect coupling of biological, hydrological, and geochemical processes and the utility of high-resolution time series of multiple solutes for understanding these linkages.

Key words: coupled elemental cycles; ecosystem stoichiometry; metabolism; nutrient assimilation; sensors; springs.

Introduction

The relatively constant nutritional requirements of organisms means they are both constrained by and alter the availability of nutrients in the environment (Sterner and Elser 2002). As organisms simultaneously respond to and alter environmental supplies of numerous elements, coupling among those element cycles occurs across levels of organization from the cell to the biosphere (Sterner and Elser 2002, Galloway et al. 2004). At the cellular level, variation among major biochemicals in the ratios of carbon (C), nitrogen (N), phosphorus (P), and other elements influences the material requirements for building organelles (e.g., ribosomes) with particular functions (Elser et al. 2000, Vrede et al. 2004). At the scale of organisms, these constraints are manifest as covariation between rates of basic biological processes (e.g., growth) and elemental composition (Elser et al. 1996, 2003). Production and maintenance of stoichiometrically homeostatic biomass, in turn, dictates that organisms acquire elements from the environment in particular proportions (Frost et al. 2005, Kerkhoff et al. 2005). In a simplified world where nutrient dynamics are controlled solely by assimilation, the timing and magnitude of inorganic nutrient uptake at the ecosystem-level should reflect those constraints.

Manuscript received 30 August 2012; revised 21 December 2012; accepted 7 January 2013. Corresponding Editor: W. V. Sobczak.
[4] E-mail: mjc@ufl.edu

In reality, the stoichiometry of ecosystem-scale nutrient dynamics is complicated by processes that weaken links between growth and assimilation, by multi-scale spatial and temporal variation in nutrient availability, and by the indirect effects of metabolism on other processes (e.g., geochemical and redox reactions; Fig. 1 [Schade et al. 2005]). At short time scales, luxury uptake may decouple assimilation from growth (Khoshmanesh et al. 2002). Over longer time scales, organismal stoichiometry can vary in response to resource ratios (Vitousek 1982, Persson et al. 2010), as can the relative abundance of organisms with differing stoichiometric requirements (Hall 2004). In addition, heterotrophs often obtain elements from organic substrates, potentially decoupling demand for various inorganic nutrients (Elser and Urabe 1999, Makino et al. 2003). Moreover, the metabolism of primary producers may influence supplies of organic matter and thus heterotrophic metabolism, including dissimilatory processes (e.g., denitrification and dissimilatory nitrate reduction to ammonia [Burgin et al. 2011]) with distinctive stoichiometry (Zarnetske et al. 2011). Metabolism also responds to and in turn influences physical and chemical conditions that control geochemical reactions (Fig. 1; see also Nimick et al. 2011). The complex interactions among these processes at various spatial and temporal scales present a challenge for understanding the influence of stoichiometric constraints on ecosystem processes, as does the limited number of tools for direct observation of stoichiometric coupling at the ecosystem level.

Lotic systems provide unique opportunities to understand general ecosystem behavior (Fisher 1997). The study of coupled element cycles, in particular, is facilitated by the downstream transport of solutes, which separates the products of ecosystem metabolism and geochemical interactions (e.g., mineral nutrient removal) from the inputs that potentially constrain them. This characteristic of flowing water enabled early development of approaches for estimation of whole-ecosystem metabolism (gross primary production and ecosystem respiration) from variation in dissolved oxygen (DO) concentrations (Odum 1956). More recent advances based on this approach have provided insights into the metabolic variation and controls across diel, successional, seasonal, and interannual time scales (Roberts et al. 2007) that have proven difficult to replicate in other ecosystems. Similarly, the concept and formalization of nutrient spiraling has provided quantitative insight into the interplay between nutrient transformations and hydrologic transport (Newbold et al. 1981). The ability to measure both ecosystem metabolism and nutrient dynamics at comparable temporal scales for whole stream ecosystems has provided elegant demonstrations of the direct coupling between nitrogen cycling and metabolism (e.g., Hall and Tank 2003, Roberts and Mulholland 2007, Hall et al. 2009). Streams have also provided more nuanced understanding of the indirect effects of metabolism on N assimilation and denitrification (Hoellein et al. 2007, Arango et al. 2008, Mulholland et al. 2008), as well as the coupling of N and P cycles (Cross et al. 2005, Schade et al. 2011).

Phosphorus (P) is a critically important element for a variety of biochemical processes, and, because of relative geogenic scarcity, one often in limited supply in freshwaters (Healey 1973, Schindler 1977, Smith 2003). Consequently, the availability of P often constrains primary production (Elser et al. 2007), and patterns of primary production likewise affect the concentrations of P in the water (e.g., Hill et al. 2001). Intentional enrichment of P for increased agricultural yields has led to widespread eutrophication of freshwater and coastal ecosystems (Bennett et al. 2001).

Despite the ecological importance of P, the tools available for understanding its fate and effects in flowing water ecosystems are limited. The P cycle is complicated by numerous geochemical interactions (House 1990, Diaz et al. 1994, Reddy et al. 1999), including redox sensitive reactions with iron and manganese, pH-sensitive co-precipitation reactions with calcium and magnesium, and sorption to/desorption from a variety of mineral and organic surfaces. In addition, the absence of a stable isotope precludes the use of methods now widely employed to understand lotic N cycling, while costs and permitting constraints severely limit the scale and resolution of radioisotope studies (e.g., Newbold et al. 1983, Tate et al. 1995). Emerging methods using enrichment dosing may permit instantaneous evaluation of gross uptake kinetics (Covino et al. 2010), but cannot partition between biotic and geochemical removal pathways, and are as limited as conventional spiraling approaches for measuring diel, event-driven, seasonal and interannual variability.

The fine-scale temporal dynamics and covariation of solutes have the potential to provide unique insight into the geophysical and ecological dynamics of watersheds, including their terrestrial and aquatic components (Kirchner et al. 2004). Recent technological developments, primarily of in situ sensors, have dramatically expanded the suite of solutes that can be observed at high frequencies over long durations. These capabilities have proven particularly valuable for evaluating not only controls and dynamics of watershed-scale nutrient export and loading (e.g., Chapin et al. 2004, Pellerin et al. 2009, 2012), but also transformations of nutrients and minerals within aquatic ecosystems. In particular, the strong influence of aquatic metabolism on diel variation of multiple solutes provides a means to understand timescales of coupling between biogeochemical processes (Nimick et al. 2011). Building on previous work describing diel NO_3 signals (Rusjan and Mikos 2010), and correlations between the magnitude of DO and NO_3 variation (Roberts and Mulholland 2007), Heffernan and Cohen (2010) demonstrated that diel NO_3 dynamics could provide quantitative inference of N assimilation that matched expected rates based on

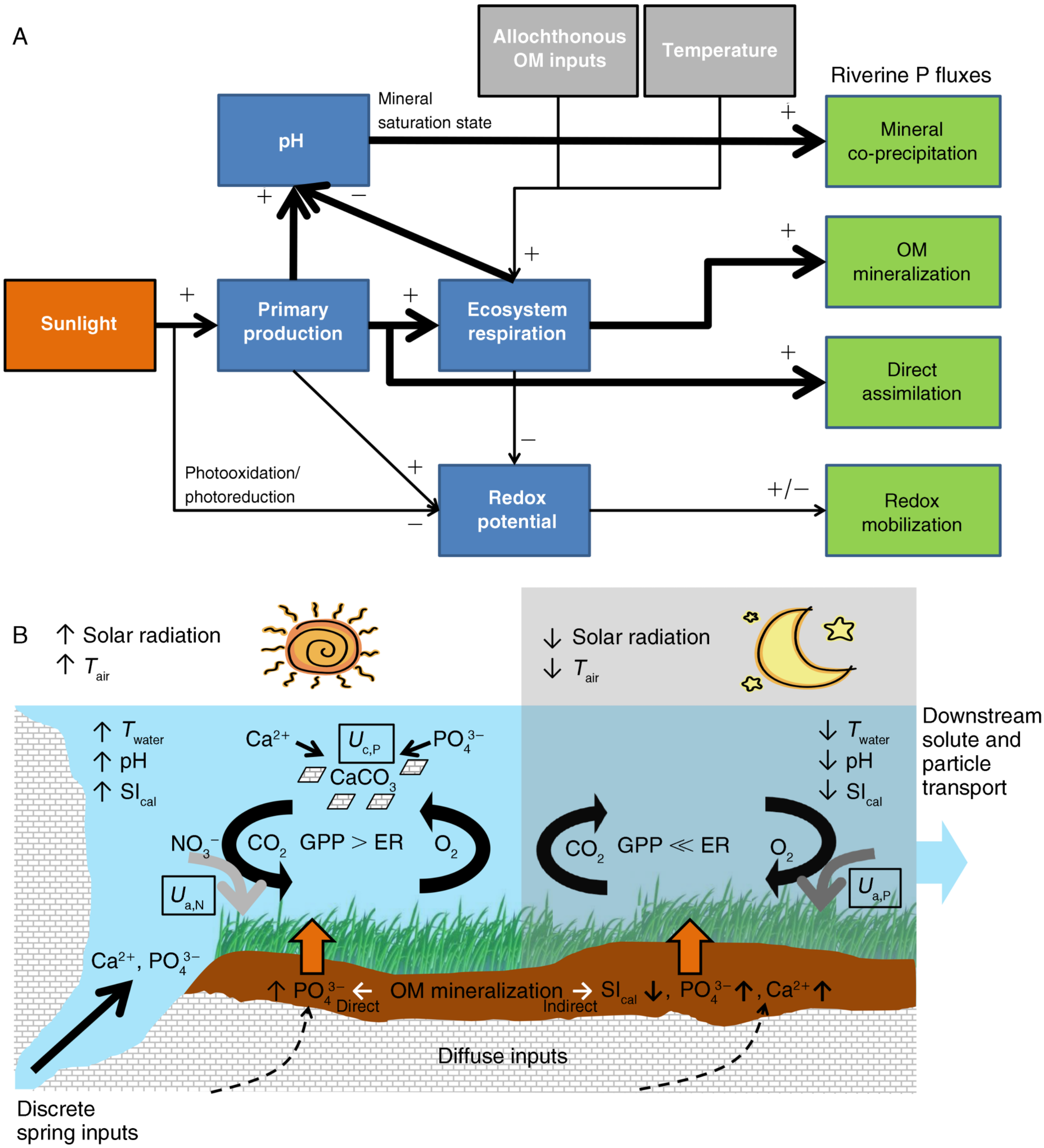

FIG. 1. Conceptual schematics showing pathways of P retention and release in rivers. (A) Numerous processes impact riverine P fluxes over diel time scales and are influenced by exogenous inputs (allochthonous organic matter [OM] and/or temperature [T]) and riverine metabolism, both directly and indirectly. Pathways are shown with signs indicating the direction of association (e.g., gross primary production [GPP] positively controls P assimilation directly, and mineral co-precipitation indirectly). The pathways explicitly quantified in this work are shown as thick lines; pathways that are likely to be of importance in other systems, but were negligible here, are shown as thin lines. (B) A schematic of the diurnally varying processes controlling P dynamics in the alkaline waters of the Ichetucknee River, Florida, USA, illustrating co-precipitation with calcite ($U_{c,P}$) during the day (when photosynthesis [GPP] increases water pH and raises the calcite saturation state, SI_{cal}), and direct autotroph assimilation ($U_{a,P}$), shown occurring at night. Also shown is the assimilation of nitrogen ($U_{a,N}$), which occurs in phase with autotroph assimilation of inorganic C (U is benthic uptake rate). The figure shows two P release pathways in response to OM mineralization in the sediments: direct release of P within the mineralized OM and indirect soluble reactive phosphorus (SRP) release via OM mineralization effects on SI_{cal}, which leads to dissolution of mineral-phase $CaCO_3$ and release of co-precipitated P. The signals of these multiple pathways are detected in the downstream fluxes of water and solutes. ER stands for ecosystem respiration.

stoichiometry and metabolism of primary producers. Moreover, the extended duration of high-frequency measurements enabled detection of day-to-day effects of primary production on subsequent denitrification. Likewise, Liu et al. (2008) and de Montety et al. (2011) used high-resolution measurements of temperature, specific conductance, and pH to document the diel dynamics of calcite precipitation–dissolution reactions in karst systems, which, in turn, exerts an important influence on numerous element cycles. This emerging capacity to disentangle the interactions between autotrophic, heterotrophic, and geochemical removal pathways illustrates the potential of in situ sensing of multiple solutes to address fundamental questions about ecosystem dynamics.

In this work, our objective was to understand controls on fine-scale variation in P fluxes and concentrations in a large spring-fed river (Ichetucknee River, Florida, USA), which we view as a model system for the inference of similar processes (albeit with varying relative importance of different pathways) in river ecosystems more broadly. To that end, we extended the diel method for inference of ecosystem-scale C–N coupling (Heffernan and Cohen 2010) to P using hourly observations of soluble reactive P (SRP) along with solutes that permit estimation of metabolism and N assimilation. In so doing, it was necessary to consider and adjust for temporally overlapping geochemical reactions missing from N cycles, which are themselves indirectly controlled by ecosystem metabolism. We hypothesized that short time scale P dynamics are jointly controlled by direct autotrophic assimilation and indirect effects of metabolism on geochemical retention pathways. This leads to three predictions: first, that autotrophic SRP assimilation will be positively correlated with GPP; second, that the strength of this association will improve after estimating and adjusting for geochemical retention; and third, that observed elemental ratios of ecosystem metabolism will correspond to measured tissue stoichiometry of dominant autotrophs.

Methods

Site description

The Ichetucknee River in north Florida is primarily fed by six large artesian springs emerging from the Floridan Aquifer. Approximately 5 km of the river (benthic area ~15.7 ha) flows through Ichetucknee Springs State Park, which extends from the most upstream springs to the downstream flow gage at the US27 bridge, and represents our study area. Like most Floridan Aquifer springs, the springs of the Ichetucknee River have extremely stable discharge, temperature, and solute chemistry (Odum 1957, Martin and Gordon 2000, Heffernan et al. 2010*a*). Fluxes of both N and P are dominated by mineral forms: NO_3 represents >90% of N flux, with concentrations ranging from 250 to 880 μg NO_3-N/L across springs, while soluble reactive phosphorus (SRP) represents >95% of total P, with concentrations between 35 to 65 μg P/L. Spring water emerges oversaturated with CO_2 (de Montety et al. 2011), and undersaturated with DO (Heffernan and Cohen 2010). Spring water is also exceedingly clear (Duarte et al. 2010), with negligible inputs and only modest longitudinal accumulation of dissolved organic matter, facilitating high primary production and dense beds of both vascular plants (principally *Sagittaria kurziana* and *Vallesnaria americana*) and filamentous benthic algae (principally *Lyngbya wollei* and *Vaucheria* spp. [Kurz et al. 2004]).

Discharge from each of the six main springs and the river at US27 was obtained from the USGS through June 2010, when all gages except Blue Hole (the largest) and the US27 bridge were discontinued. For subsequent deployments, regressions between archived flow at each spring (prior to June 2010) and flows at Blue Hole and US27 were used to reconstruct more recent daily discharge; regressions for each spring predicted over 70% of spring-flow variation. Previous work summarizing gage estimated flows (Heffernan et al. 2010*a*) suggests that spring inputs exceed downstream river flow by an average of 10%. However, continuous measures of hydraulic head gradients at multiple locations in the river suggest persistent gaining conditions (de Montety et al. 2011; M. J. Kurz, J. B. Martin, and M. J. Cohen, *unpublished manuscript*), consistent with the presence of small springs and seeps along the entire river. Because of high inherent uncertainty in spring-vent discharge estimates, we use measured spring flows only to estimate flow-weighted nutrient concentrations. We estimated nutrient mass fluxes for reach scale mass balances as the product of flow-weighted concentrations from the major springs and measured river discharge at the downstream gage.

Sensors and deployments

We co-deployed three in-situ sensors in the advective zone of the Ichetucknee River at the downstream location during eight multi-day deployments between September 2009 and May 2011 (Table 1). Deployments were generally a week or more (mean = 10 days, range from 6 to 15 days), but data for full diel cycles for inference of metabolism and assimilation were not available on the first or last day. Deployments spanned all but the summer months, when intensive recreation on the Ichetucknee River precluded sensor installation and retrieval.

At hourly resolution during each deployment, we measured temperature (T), specific conductance (SpC), and optical dissolved oxygen (DO) using a multiparameter sonde manufactured by Yellow Springs Instruments (6920 V2; YSI, Yellow Springs, Ohio, USA). Nitrate (NO_3) was measured every 15 minutes using a submersible UV nitrate analyzer (SUNA; Satlantic, Halifax, Nova Scotia, Canada) operated in "polled" mode wherein a burst of 20 NO_3 measurements were obtained at each sampling interval and averaged;

TABLE 1. Summary of sensor deployment dates and ambient river, spring, and atmospheric conditions during each deployment.

Date	Duration (d)	Discharge (m^3/s)		Springs FW (μg/L)		Mean solar radiation ($W \cdot m^{-2} \cdot d^{-1}$)	T_{air} (°C)
		River	Springs†	SRP	NO_3		
2009							
Sep	10	7.3	7.6	48	580	4275	31.5/21.3
2010							
Apr	15	8.9	8.3	46	‡	4987	25.9/11.6
May	11	9.3	8.5	47	605	5896	31.3/19.1
Oct	6	8.2	7.7	49	612	4590	28.0/11.3
Dec	15	7.9	7.4	53	601	2730	15.6/0.8
2011							
Feb	6	7.7	7.9	50	607	2082	14.3/5.7
Mar	9	8.0	8.1	49	613	4490	24.4/11.5
May	7	7.8	7.4	49	609	6191	27.7/14.1

Notes: FW refers to flow weighted input concentrations of both soluble reactive phosphorus (SRP) and NO_3. T_{air} is air temperature; maximum and minimum values are given.

† Discharge measurements were discontinued on four of six springs in June 2010. Values prior to this date are measured, and values after are estimated based on covariance relationships with remaining gages (Blue Hole, river discharge at US27 Bridge).

‡ The submersible UV nitrate analyzer (SUNA) failed; spring N inputs were not recorded.

the SUNA failed to obtain usable data during the April 2010 deployment. Within-burst variation was small (CV $< 3\%$), particularly compared with observed systematic variation. Sensor estimates of NO_3 were previously validated vs. discrete field measurements and laboratory variation experiments (Heffernan and Cohen 2010), and between-deployment variation was removed using baseline absorbance measurements in deionized water prior to each deployment. The SUNA was equipped with a copper guard and wrapped in 100-μm Nitex screening to prevent biofouling. Low turbidity and dissolved organic matter permitted measurements without further correction. Finally, we deployed an in situ phosphate sensor (Cycle-PO4; Wetlabs, Philomath, Oregon, USA), which uses the ascorbic acid method (EPA365.1) to estimate SRP. Aliquots of river water were pumped through 0.45-μm filters before mixing with reagents and reacting for 17 minutes. An LED light source at 870 nm and detector measure colorimetric response across a 5-cm path length; on-board standards are used for internal calibration. The instrument has a range of 0–310 μg P/L, and a lower detection limit of 2.3 μg P/L. Laboratory tests with standards run as unknowns suggest high accuracy (bias < 5 μg P/L) and precision (2 vs. 1.5 μg P/L) comparable with manufacturer specifications.

On three occasions (26 March 2009, 2 November 2009, and 10 May 2011), we deployed an ISCO 6700 series autosampler (Teledyne Isco, Lincoln, Nebraska, USA) at the downstream location for 48 hours to obtain hourly filtered water samples. These samples were analyzed immediately for major cation concentrations to estimate [Ca^{2+}] using a Dionex DX-500 ion chromatograph (Thermo Fisher Scientific, Waltham, Massachusetts, USA) in the Hydrogeochemistry Lab at the University of Florida. Measured [Ca^{2+}] concentrations were regressed against simultaneous measurements of SpC from our field sondes to develop a proxy relationship that could be used to estimate [Ca^{2+}] during all other deployments. At the outset of each deployment, we obtained filtered water samples from each of the six main spring vents that were analyzed for SRP using the ascorbic acid method (EPA 365.1 [Kuo 1996]) and NO_3 using second-derivative UV spectra obtained from an Aquamate UV-Vis spectrophotometer (Thermo Fisher Scientific [Simal et al. 1985]).

Metabolism and nutrient assimilation

For each deployment, we calculated gross production (GPP; g $O_2 \cdot m^{-2} \cdot d^{-1}$) and ecosystem respiration (ER; g $O_2 \cdot m^{-2} \cdot d^{-1}$) from diel DO variation using the single-station method. DO concentrations in the contributing springs ranged from 4 mg/L (Ichetucknee Head Spring) to 0.2 mg/L (Mill Pond Spring). We estimated reaeration (k) using nighttime regression between the DO saturation deficit and the hourly DO rate of change (Owens 1974). The time range for each regression varied across deployments due to differences in flow and day length but was generally between 23:00 and 03:00. Regression fits were strong (mean $r^2 = 0.97$ across deployments; range 0.88–0.99), and inferred k values consistent (0.45 $\pm$ 0.03 hr^{-1}). Because we found no systematic variation across deployments (e.g., with discharge or air temperature), but unexplained variation within deployments, we used a single k value (0.45 hr^{-1}) for all metabolism calculations. Conservative tracer tests in the Ichetucknee River (Hensley and Cohen 2012) suggest a mean residence time of 6 hours to the downstream location. Consequently, we assume the entire benthic area (15.7 ha) contributes to daily metabolism. To convert GPP to net primary production (NPP) for estimating uptake stoichiometry, we assumed a photosynthetic coefficient of 1.0 (Odum 1957) and autotrophic respiration equal to 50% of GPP (Hall and Tank 2003).

Nitrogen removal due to autotrophic assimilation ($U_{a,N}$ [mg $N \cdot m^{-2} \cdot d^{-1}$], where U is the benthic uptake rate [mass per area per time]; subscripts refer to the

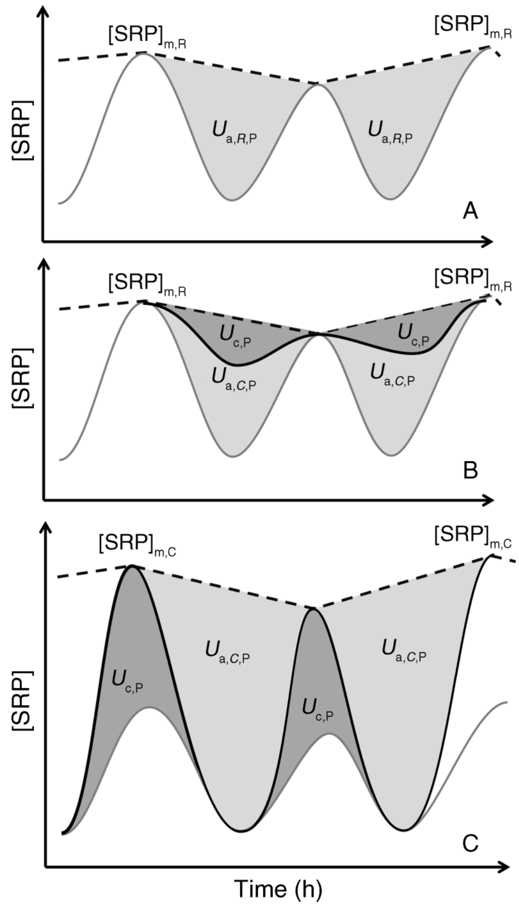

FIG. 2. Schematic of the model for estimating autotrophic P assimilation ($U_{a,P}$) from diel [SRP] variation. In all cases, P removal is evaluated as the integrated concentration difference between observations (gray line) and the interpolation (dashed line) between diel maxima ($[SRP]_m$). (A) The first model estimates assimilation from raw data uncorrected for potential geochemical effects ($U_{a,R,P}$). (B) The second model considers total removal to be the combination of assimilation ($U_{a,C,P}$) and calcite co-precipitation ($U_{c,P}$), but where both removal processes occur in phase, such that removal rates are zero at the diel maxima, which is inferred from the raw data. (C) The third model considers the combined effects of assimilation ($U_{a,C,P}$) and geochemical ($U_{c,P}$) removal when these processes occur out of phase. The result of their additive effect is to adjust the diel maxima ($[SRP]_{m,C}$) from which $U_{a,C,P}$ is estimated. With respect to model A, geochemical P removal may lead to overestimates of assimilation (model B, processes in phase) or underestimates of assimilation (model C, processes out of phase). Note that flow-weighted spring inputs are not the same as the diel maxima and may be higher (reach is a net sink) or lower (reach is a net source).

nutrient [N or P], the pathway [where a is assimilation, c is co-precipitation, and d is denitrification], and the use of raw or corrected concentrations [R is raw, C is corrected]) was estimated using the extrapolated diel method (Eq. 1 in Heffernan and Cohen 2010). Variation in the nighttime baseline $[NO_3]$ was ascribed to day-to-day variation in dissimilatory removal ($U_{d,N}$), which was estimated quantitatively using daily mass balance between spring inputs and river output (Eq. 3 in Heffernan and Cohen [2010]). Uptake of ammonium or dissolved organic N was neglected based on observed input concentrations that are below detection. We did not calculate gross heterotrophic N removal based on estimates in Heffernan et al. (2010*a*) that suggest this is negligible. All diel variation in $[NO_3]$ was assumed to be due to autotrophic uptake, with zero uptake assumed at each nighttime maxima; spring inputs were assumed constant, an assumption previously validated based on high serial autocorrelation in concentrations measurements over months. The short measured hydraulic residence time (Hensley and Cohen 2012) in the river precludes confounding effects on the $U_{a,N}$ signal from long residence time waters, a finding previously validated (Heffernan and Cohen 2010) using temperature as a tracer.

Phosphorus removal due to autotrophic assimilation ($U_{a,P}$; mg $P \cdot m^{-2} \cdot d^{-1}$) was estimated from diel SRP variation using two variants of the mass balance framework used for estimating $U_{a,N}$. Our first approach used raw observed hourly SRP concentrations ($SRP_{t,R}$) that were smoothed using a three-hour moving average; this modest smoothing was needed to attenuate noise in the signal that affects the inference of diel peaks that, in turn, is the most sensitive parameter for estimating P uptake. To test the impact of smoothing on all subsequent analyses, we compared flux rates with and without smoothing. P removal inferred using smoothing was more consistent ($CV_{sm} = 0.12$, $CV_{raw} = 0.18$), but slightly underestimated fluxes (slope = 0.97, $r^2 = 0.98$). Because smoothing markedly stabilized diel maxima estimates and introduced negligible bias, all subsequent values are reported using the smoothed data. We interpolated between sequential diel peaks ($SRP_{m,R,i}$ and $SRP_{m,R,i+1}$) to create a moving baseline, and estimated P removal (mg $P \cdot m^{-2} \cdot d^{-1}$) on each day, i, as the summed deviation of observed hourly concentrations (for time t, SRP_t) from that baseline (Fig. 2A), multiplied by discharge on that day (Q) and divided by benthic area (A):

$$U_{a,R,P,i} = \frac{Q_i}{A} \sum_{t=0}^{24} \left[SRP_{m,R,i} - \frac{t}{24} \times (SRP_{m,R,i} - SRP_{m,R,i+1}) - SRP_{t,R} \right]. \quad (1)$$

Note that we did not constrain the SRP baseline concentrations based on the spring vent inputs, reasoning that other sources (diffuse inputs) of different concentrations may be important. Moreover, diel baselines determined from the raw data are delimited as such in Fig. 2A to distinguish from the other method where the baseline is corrected for effects of geochemical interactions. Comparing daily baseline ($SRP_{m,i}$ and $SRP_{m,i+1}$) to spring vent inputs indicates whether the river is a net P source or sink.

Our second approach to estimating P uptake corrects for potential geochemical interactions between water column P and in situ production of calcite minerals in the Ichetucknee River. During these and previous deployments, we observed coherent diel variation in SpC, consistent with reduced ion activity during the day. Given that the alkalinity of the spring inflows is constant, that bicarbonate is the predominant anion in these waters, and that spring vent water is oversaturated with respect to calcite (de Montety et al. 2011), but not other minerals, this diel SpC signal implies daytime calcite precipitation. Specifically, daytime decreases were observed in SpC ranging between 6 and 15 μS/cm from a nighttime maximum that consistently matched the flow-weighted springs inputs (~338 μS/cm). Previously, de Montety et al. (2011) showed nighttime calcite equilibrium (i.e., $SI_{cal} \approx 0$) and daytime oversaturation ($SI_{cal} = 0.6$), supporting the contention that pH variation in response to photosynthetic consumption of bicarbonate (and replenishment via respiration) leads to changing mineral saturation. Resulting daytime precipitation of calcite was indicated by a diel cycle in Ca concentrations (1.34–1.40 mmol/L) that peaked at midday (de Montety et al. 2011). Notably, the river was always undersaturated with respect to other minerals that might sorb phosphate (aragonite, dolomite, and Fe oxide phases). Other mineral interactions (e.g., Fe, Mg, Al) are also possible, but were determined to be of negligible magnitude and were thus neglected. No evidence of diel Al variation has been observed, nor is any expected due to redox or temperature. Mg also exhibits muted diel variation (M. J. Kurz, V. de Montety, J. B. Martin, M. J. Cohen, and C. R. Foster, *unpublished manuscript*), but because river water is always under-saturated with respect to dolomite and magnesite, this signal is likely due principally to autotrophic uptake or co-precipitation with calcite. Diel variation in Fe was also observed, likely due to diel effects on redox that, in turn, affects Fe solubility, but the magnitude of this variation was too small (~2 μg/L; M. J. Kurz, V. de Montety, J. B. Martin, M. J. Cohen, and C. R. Foster, *unpublished manuscript*) to exert substantial control on diel SRP variation.

P co-precipitation with calcite ($U_{c,P}$) was estimated based on calcite saturation, and published sorption kinetics of PO_4 to calcite. Specifically, we used the mass transfer equations presented in Plant and House (2002) and House (1990), assuming that the adsorption kinetics of P co-precipitation are sufficiently rapid (<60-minute sampling interval [House 1990]) that they are not rate limiting. The mass of inorganic P co-precipitated per volume ($\Delta n_{P,t}$ [μmol/L]) within each hourly sampling interval, t, is computed as a function of the Avagadro constant (N_A; 6.022×10^{23} mol^{-1}), the surface density of co-precipitated phosphorus (σ, μmol/m^2), the molar area of $CaCO_3$ (δ; 20.101×10^{-20} m^2), the dissolved calcium removed via precipitation based on hourly ($n_{Ca,t}$ [μmol/L]) and daily maximum concentration ($n_{Ca,m}$ [μmol/L]), and a term, h(sol), that describes the form of the sorption isotherm given the composition of the solution (i.e., PO_4^{3-} vs. HPO_4^{2-}), temperature, pH, and published equilibrium constants:

$$\Delta n_{P,t} = N_A \times \sigma \times \delta \times h(\text{sol}) \times (n_{Ca,m} - n_{Ca,t}). \quad (2)$$

Ion activity data (de Montety et al. 2011; M. J. Kurz, V. de Montety, J. B. Martin, M. J. Cohen, and C. R. Foster, *unpublished manuscript*) support the assumption that the unprotonated form of phosphate (PO_4^{3-}) is negligible in the alkaline waters of the Ichetucknee; this collapses the h(sol) term from House (1990) to a simple ratio based only on the SRP concentration and an adsorption constant for protonated phosphate (K_2 constant = 0.99967). Eq. 2 also assumes constant temperature, which is tenable in this stable thermal environment. Finally, we assumed a surface density of co-precipitated P (σ = 0.055 μmol/m^2) observed in a chalk river (River Frome, Dorset, UK [House 1990]). Idealized laboratory experiments generally yield higher values (~0.150 μmol/m^2), but these may not accurately represent the more complex surface chemical reactions in environmental settings; co-precipitation fluxes are particularly sensitive to this surface density parameter. We estimated co-precipitation retention ($U_{c,C,P}$) by integrating hourly concentration effects ($\Delta n_{P,t}$) multiplied by discharge and divided by benthic area.

Co-precipitation does not necessarily occur in phase with autotroph assimilation, and could cause over- or underestimation of assimilation based on its diel variation. Our approach to extracting the magnitude of assimilation from the convolved signal of uptake and co-precipitation was to adjust measured SRP concentrations in the river by adding the estimated co-precipitation effect on concentration. If the two processes are exactly in phase, and (as assumed) exert no effect on water column concentrations at their diel maxima (i.e., SRP_m is the same in Fig. 2A and B), interpreting the raw diel signal as assimilation alone will be an overestimate (Fig. 2B). If, however, the processes are out of phase (Fig. 2C), their additive effects will change both the geometry and baseline values of the diel signal. The greater the phase difference, the more the observed diel amplitude will be muted and lead to an underestimate of the assimilatory flux by shifting the SRP diel baseline ($SRP_{m,C}$; Fig. 2C). By adding estimated calcite co-precipitation to the raw SRP signal, we extracted the diel signal that would have been present had assimilation been the only process operating ($SRP_{t,C}$). Assimilation is estimated using the Eq. 1 formulation, but with $SRP_{t,C}$ for hourly measurements and $SRP_{m,C}$ as the daily baseline:

$$U_{a,C,P,i} = \frac{Q_i}{A} \sum_{t=0}^{24} \left[SRP_{m,C,i} - \frac{t}{24} \times (SRP_{m,C,i} - SRP_{m,C,i+1}) - SRP_{t,C} \right]. \quad (3)$$

The above formulation makes two important assumptions that we investigate using correlative evidence. First, it permits the presence of day-to-day variation in the diel baseline. Observed variation in [NO_3] baseline (Heffernan and Cohen 2010) was interpreted as day-to-day changes in dissimilatory fluxes, but such pathways are not part of the P cycle. The stability of spring vent flow (monthly serial autocorrelation of +0.88) and chemistry (CV < 9% from archival SRP measurements) further suggests that any day-to-day variation is not due to variation in sources. The mechanisms that induce SRP baseline variation between days and deployments are unknown, but may be related to the magnitude of benthic respiration (Kleeburg and Schlungbaum 1993), hyporheic exchange (Mulholland et al. 1997), calcite co-precipitation ([de Montety et al. 2011] which is, itself, varying from day to day), and discharge. The second embedded assumption is that inputs (i.e., SRP_m) are not bounded by spring vent concentrations. Two mechanisms may enrich nighttime concentrations vis-à-vis the spring vents. First, mineralization of organic P, which we assume is diurnally constant, would deliver P to the river reach such that nighttime concentrations could be slightly elevated above flow-weighted spring inputs. Second, diffuse seepage to the river, which was estimated to be ~1 m^3/s based on a chloride budget of the river (de Montety et al. 2011), may constitute an important flux. Previous efforts to develop reach-scale N mass balance could safely neglect this flux because porewater measurements suggest complete denitrification of water upwelling through the river sediments, but those measurements suggest high SRP concentrations (~150 μg P/L [M. J. Kurz, J. B. Martin, and M. J. Cohen, *unpublished manuscript*]).

Statistical analysis

We used ordinary least squares regression to evaluate covariance between specific conductance and [Ca] to build proxy relationships for P co-precipitation fluxes. For both raw and corrected [SRP] estimates of assimilation, we regressed net primary production against $U_{a,P}$. Goodness-of-fit and slope were both used to contrast the different methods of estimating $U_{a,P}$, noting that the slope when C and P assimilation are reported on a molar basis is the C:P stoichiometry of ecosystem metabolism. A similar approach for ecosystem C:N stoichiometry using $U_{a,N}$ was also adopted. Variation in SRP_m within and across deployments was evaluated against estimates of heterotrophic processes (ecosystem respiration, ER; denitrification, $U_{d,N}$) as well was measured discharge. To correct for the effects of spring inputs, we calculated the deviation of the daily baseline from the flow weighted spring inputs (i.e., $\Delta SRP_m = SRP_m - SRP_{spr}$). Theory predicts an inverse relationship (i.e., negative Pearson correlation coefficient) between GPP and ecosystem stoichiometry, resulting from higher algal contribution during periods of higher GPP, which we evaluated using linear regression for both C:N and C:P. We compared the inferred ecosystem stoichiometric ratios with measured tissue ratios of the dominant autotroph taxa to indicate the relative contribution of algae vs. vascular plant to ecosystem primary production. Finally, we investigated the temporal patterns of autotrophic processes using biplots of concentration. Of particular interest were lag patterns between dissolved oxygen dynamics (with a peak in mid- to late-afternoon each day) and diel variation in [Ca], [NO_3], and [SRP] (both raw and corrected).

Results

Discharge conditions varied over the eight deployments, ranging both above and below the long-term mean discharge of 8.3 m^3/s. During these deployments, gage-measured river discharge (at the US27 bridge) was higher than cumulative spring-vent flows, and there was a strong positive correlation between river flows and hydrologic deficit (river minus springs; $r = 0.81$, $P = 0.01$), suggesting systematic variation in diffuse water delivery. Spring vent chemistry was stable, with flow-weighted concentrations of SRP at 48.8 ± 2.1 μg P/L and NO_3 at 604 ± 11.3 μg N/L (mean ± SD). There was a negative correlation between spring vent flows and flow-weighted [SRP] ($r = -0.69$, $P = 0.06$). Variation in solar forcing also varied dramatically across deployments. Peak primary production in these rivers is typically in late spring (April–June) prior to full leaf out of the riparian canopy, and peak radiation is delivered during this relatively cloud-free period. Numerous storm days were sampled, during which solar radiation was substantially reduced, with commensurate effects on diel solute cycles.

From three autosampler deployments (March 2009, November 2009, May 2011), we obtained a strong predictive relationship between specific conductance (SpC) and measured [Ca] (Fig. 3). While the intercepts in each case were slightly different, the slopes converged on a consistent value of 0.0041 $mmol \cdot L^{-1} \cdot cm^{-1} \cdot \mu S^{-1}$, which we used throughout all deployments to estimate [Ca] from measured SpC. Notably, the covariance between [Ca] and SpC was strongest with a 2-hour lag in all cases. That is, changes in [Ca] were slightly out of phase with SpC, possibly because of the influence exerted on SpC by other ions (e.g., Mg) that are out of phase with Ca. This lag was propagated throughout all subsequent calculations for estimating calcite co-precipitation of SRP.

Regular diel variation was observed for DO, [NO_3], SpC, and [SRP], although the magnitude of the diel cycles varied considerably (e.g., March 2011, Fig. 4; December 2010, Fig. 5). Diel cycles were relatively symmetrical for DO, SpC, and NO_3, although nighttime concentrations of DO and NO_3 were nonstationary. In contrast, the raw SRP signal (gray lines in Figs. 4C and 5C) was clearly asymmetrical, with consistent evidence of a midday change in slope, particularly in the March

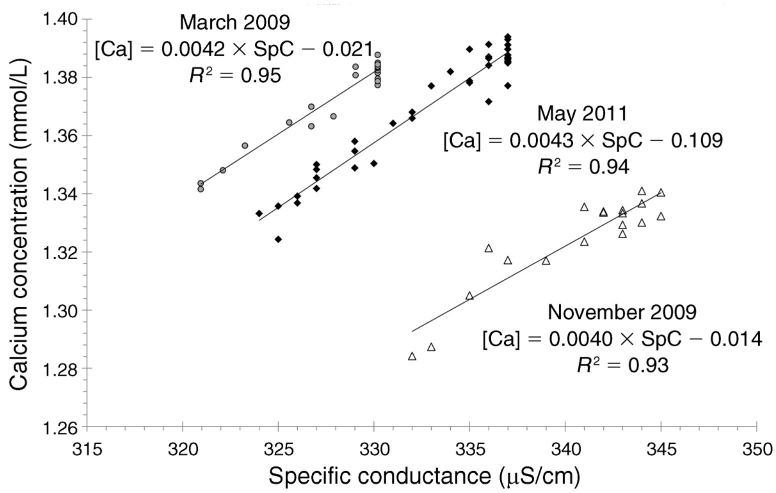

FIG. 3. Covariance between specific conductance (SpC) and measured [Ca] during three 36-hour auto-sampler deployments. The fitted slope was used to estimate diel variation in [Ca] from SpC during all deployments, which allows estimates of P co-precipitation. Note that the fitted line was, in each case, best fit when accounting for a short (~1–2 hour lag) between changes in [Ca] and resulting changes in SpC.

2011 deployment (Fig. 4). For all deployments, the measured downstream [SRP] was greater than the flow-weighted spring inputs except for a few hours near midnight (Fig. 4) suggesting an additional source of P to the Ichetucknee River. In contrast, N is always removed from Ichetucknee River, albeit with net removal efficiencies varying diurnally and between deployments; springs N inputs are ~0.61 mg N/L (data not shown in Figs. 4 and 5) while downstream concentrations vary between 0.3 and 0.45 mg N/L.

Across all deployments, the timing of the diel maxima for solar radiation and DO and the diel minima for SpC, NO_3, and SRP were relatively consistent (Table 2). Radiation peaked near noon each day, and DO peaked 3–4 hours later. The fine-scale variation of NO_3, SpC, and SRP (both raw and corrected for calcite co-precipitation) vs. DO for the March 2011 deployment (Fig. 6) indicates varying lag patterns. As has been previously observed in this river (Heffernan and Cohen 2010), [NO_3] maxima occurred just before dawn, and minima at the same time as peak DO (approximately 15:00; Fig. 6A); the absence of any diel hysteresis between DO production and NO_3 removal suggests no N assimilation lag. SpC declined with autotrophic consumption of bicarbonate (and other ions) and reached its minima slightly before DO (2–3 hours after the radiation peak; Fig. 6B). Of particular note was the consistent observation that the SRP minima occurred just before midnight, lagging solar radiation by 10–12 hours, and DO by 8–9 hours (Fig. 6C and D). Marked asymmetry in the raw diel SRP signal is clearly evident (Fig. 6C), but absent in the calcite-adjusted signal (Fig. 6D). There was no apparent relationship between discharge and the timing of the diurnal signal, nor of discharge with the lag behind peak radiation. However, we did observe a consistent positive association for observed peak timing between DO, SpC, and NO_3 (mean $r = 0.58$), which also held for observed lag behind peak radiation (mean $r = 0.68$). SRP operated apparently independently of the other diel cycles, and was significantly correlated ($r = 0.74$, $P = 0.04$) only with day length (longer days led to later minima). Because peak radiation was relatively consistent around noon, this covariance may suggest that the diel SRP minima are partially controlled by the timing of sundown.

We observed a wide range of stream metabolism conditions over the eight deployments (Table 3), with deployment mean GPP varying between 6.6 ± 1.8 (mean ± SD; February 2011) and 18.1 ± 1.1 (May 2010) g $O_2 \cdot m^{-2} \cdot d^{-1}$ and ER between 9.1 ± 0.4 (December 2010) and 13.6 ± 0.1 (May 2010) g $O_2 \cdot m^{-2} \cdot d^{-1}$. GPP and ER were strongly correlated ($r = 0.91$, $P < 0.001$), but because GPP varied more than ER ($SD_{GPP} = 4.4$ vs. $SD_R = 1.8$ g $O_2 \cdot m^{-2} \cdot d^{-1}$), the river fluctuated between consistent net autotrophy in spring deployments (GPP : ER ≈ 1.3 ± 0.1) and weaker but still consistent net heterotrophy in fall and winter deployments (GPP : ER ≈ 0.8 ± 0.1). Spanning all measurement dates, GPP was well-predicted by daily incident radiation ($r^2 = 0.65$, $P < 0.001$), while respiration was more weakly but still significantly predicted by minimum daily water temperature ($r^2 = 0.35$, $P \leq 0.001$).

Estimates of N assimilation ($U_{a,N}$) and denitrification ($U_{d,N}$) ranged widely across deployments (Table 3). $U_{a,N}$ was predicted by GPP across ($r^2 = 0.90$, $P < 0.001$), and within (mean $r^2 = 0.64$) deployments. $U_{d,N}$ varied over a wide range (430–1190 mg $N \cdot m^{-2} \cdot d^{-1}$), but was far more regular within each deployment than $U_{a,N}$ ($CV_{Ua} = 0.19$, $CV_{Ud,N} = 0.07$). As expected, U_{den} was predicted by ecosystem respiration ($r^2 = 0.69$, $P < 0.001$) and accounted for, on average 85 ± 4% of net N removal

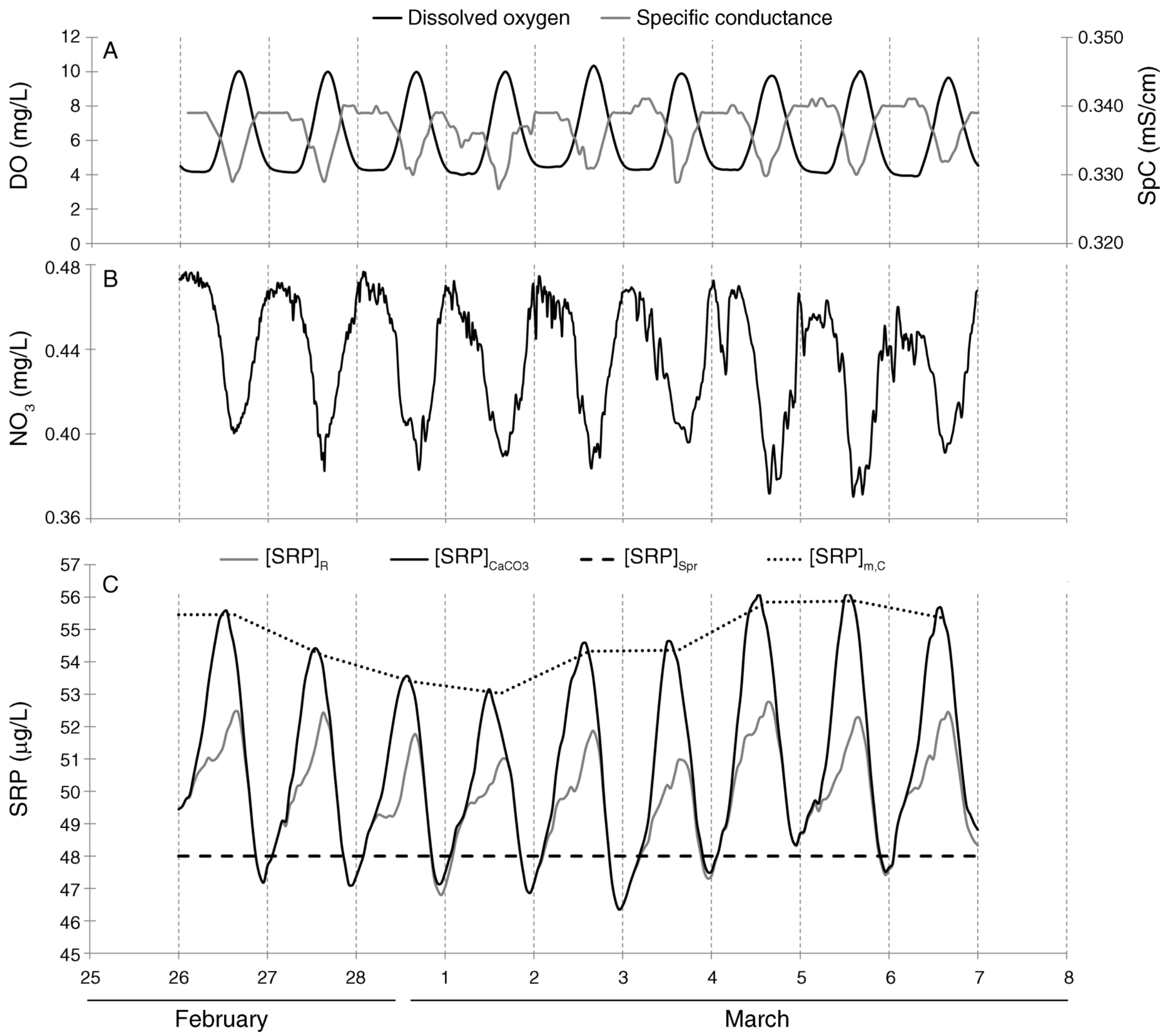

FIG. 4. Diel signal during March 2011 deployment for (A) dissolved oxygen and specific conductance, (B) [NO_3], and (C) raw ([SRP]$_R$) and co-precipitation corrected [SRP] ($CaCO_3$ corrected [SRP]$_{CaCO3}$; springs input, [SRP]$_{spr}$; maximum corrected [SRP]$_{m,C}$). The horizontal dashed line in panel C is the flow-weighted inputs of the springs, and the dotted line is the diel maximum (baseline) used to estimate assimilation. Vertical dashed lines denote midnight of each day of the deployment. During the deployment, the reach was a modest source of P.

($U_{tot,N}$) and 29% ± 7% (mean ± SD) of spring-vent N inputs.

Estimated co-precipitation of P with calcite significantly affected the diel variation in SRP concentrations (Figs. 4C and 5C). Raw diel SRP variation and predicted P removal via co-precipitation were out of phase, with the diel minima lagging peak predicted co-precipitation by 8–9 hours. At night, when calcite co-precipitation drops to zero, the grey line (raw [SRP]) and black line (corrected [SRP]) converge. Adjusting raw SRP data for calcite co-precipitation alters the diel signal to be more symmetrical (Fig. 6C vs. 6D), suggesting the raw signal results from the convolution of two signals: autotrophic assimilation and calcite co-precipitation. Correcting the raw SRP signal for co-precipitation (black lines, panel C in Figs. 4 and 5) increases the daily baseline concentration (SRP_m), which, in turn, alters estimates of P assimilation.

Our estimates of autotrophic P assimilation were significantly predicted by GPP using raw vs. calcite co-precipitation corrected SRP concentrations (Fig. 7), but using raw [SRP] yielded a weaker association ($r^2 = 0.53$, $F_{1,68} = 73$) than using corrected [SRP] ($r^2 = 0.84$, $F_{1,68} = 381$). The fraction of total P removal due to assimilation made after adjusting for calcite co-precipitation ($U_{a,C,P}$) was relatively constant across deployments at 70% ± 9%. However, variation in the magnitude of assimilatory removal across deployments was large (mean $U_{a,C,P}$ ranged from 6.4 ± 1.6 to 20.9 ± 2.3 mg $P \cdot m^{-2} \cdot d^{-1}$), with the highest values observed during spring deployments (Table 3). Variation in within deployment mean P-removal via co-precipitation

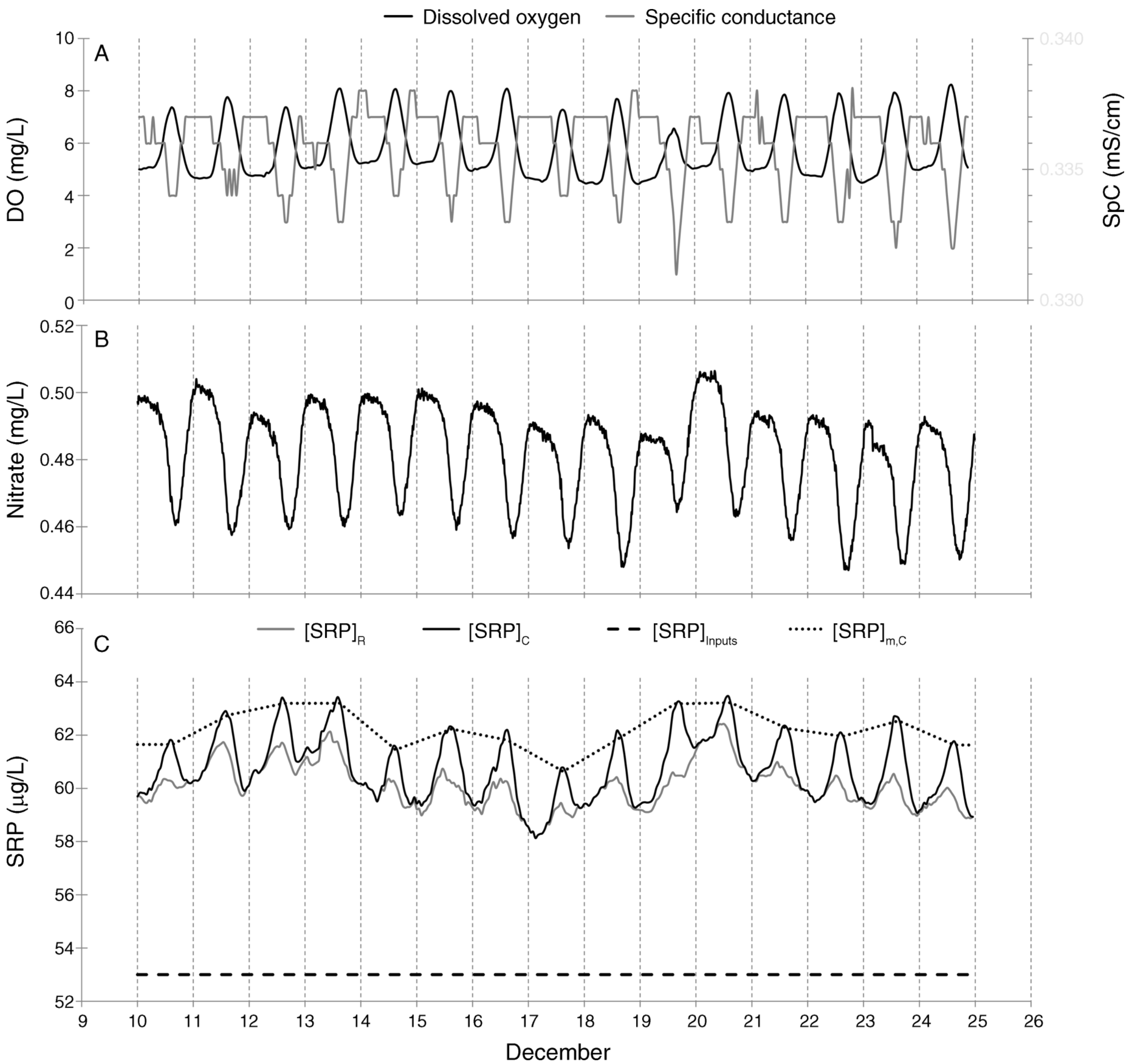

FIG. 5. Diel signal during December 2011 deployment for (A) dissolved oxygen and specific conductance, (B) [NO_3], and (C) raw and co-precipitation corrected [SRP]. The horizontal dashed line in panel C indicates the flow-weighted inputs of the springs, and the dotted line is the diel maximum (baseline) used to estimate assimilation. Vertical dashed lines denote midnight of each day of the deployment. Note the dramatic increase in SRP between the springs and the downstream location suggesting that the 5-km reach is a significant source during this deployment.

($U_{c,P}$) was almost as large (2.7 ± 0.9 to 8.0 ± 1.6 mg $P \cdot m^{-2} \cdot d^{-1}$), and was strongly correlated with GPP as well ($r = 0.71$, $P < 0.001$; data not shown), as expected since metabolism is an important control on pH and calcite saturation in the river.

Differences between $U_{a,R,P}$ and $U_{a,C,P}$ were primarily attributable to the effect of calcite correction on SRP_m. The difference between $SRP_{m,R}$ and $SRP_{m,C}$ was strongly correlated with GPP ($r = 0.88$, $P < 0.001$), underscoring that production affects both co-precipitation ($U_{c,P}$; indirectly) and assimilation ($U_{a,C,P}$; directly). Variation in SRP_m was considerable across deployments (Table 3) and even within deployments (Figs. 4 and 5). Of particular note is the deviation of SRP_m from the flow-weighted springs inputs (ΔSRP_m; Table 1). $\Delta SRP_{m,}$ after co-precipitation correction, was correlated with both ecosystem respiration (ER) and flow (Q; Fig. 8). Strong covariance between these two potential control variables ($r = 0.89$, $P < 0.001$) resulted in limited additional explanatory power when they were combined in a multiple regression ($r^2 = 0.79$, $P < 0.001$), but both were statistically significant predictors (for ER, $P = 0.005$; for Q, $P < 0.001$). No model explained much of the within-deployment variation in SRP_m, the source of which remains unresolved.

The slope of each association (Fig. 8) indicates ecosystem-scale autotrophic stoichiometry; adjusting fitted slopes to a molar basis and conversion of GPP

TABLE 2. Flow rate (Q) and timing of diel cycle maxima (max., for DO and radiation) and minima (min., for NO_3, SpC, and SRP).

Date	Q (m^3/s)	DO max.	NO_3 min.	SpC min.	SRP min.	Radiation max.	Day length
2009							
Sep	7.2	15.1	14.6	14.3	23.9	12.3	12.4
2010							
Apr	8.9	15.7	‡	15.1	23.6	12.3	12.7
May	9.3	15.1	14.4	14.4	23.7	12.5	13.6
Oct	8.2	15.8	14.5	14.5	23.5	11.5	11.2
Dec	7.9	15.7	16.9	15.4	23.1	12.3	10.3
2011							
Feb	7.7	15.6	15.8	14.8	23.3	11.7	11.0
Mar	8.0	16.0	15.6	14.4	23.2	12.8	11.9
May	7.8	16.4	15.5	15.2	23.6	12.6	13.3

Notes: All times are reported in decimal hours using Eastern Standard Time. Day length is the duration of positive measured insolation. Abbreviations are: DO, dissolved oxygen; NO_3, nitrate; SpC, specific conductance; SRP, phosphate.
‡ SUNA failed; no NO_3 data collected.

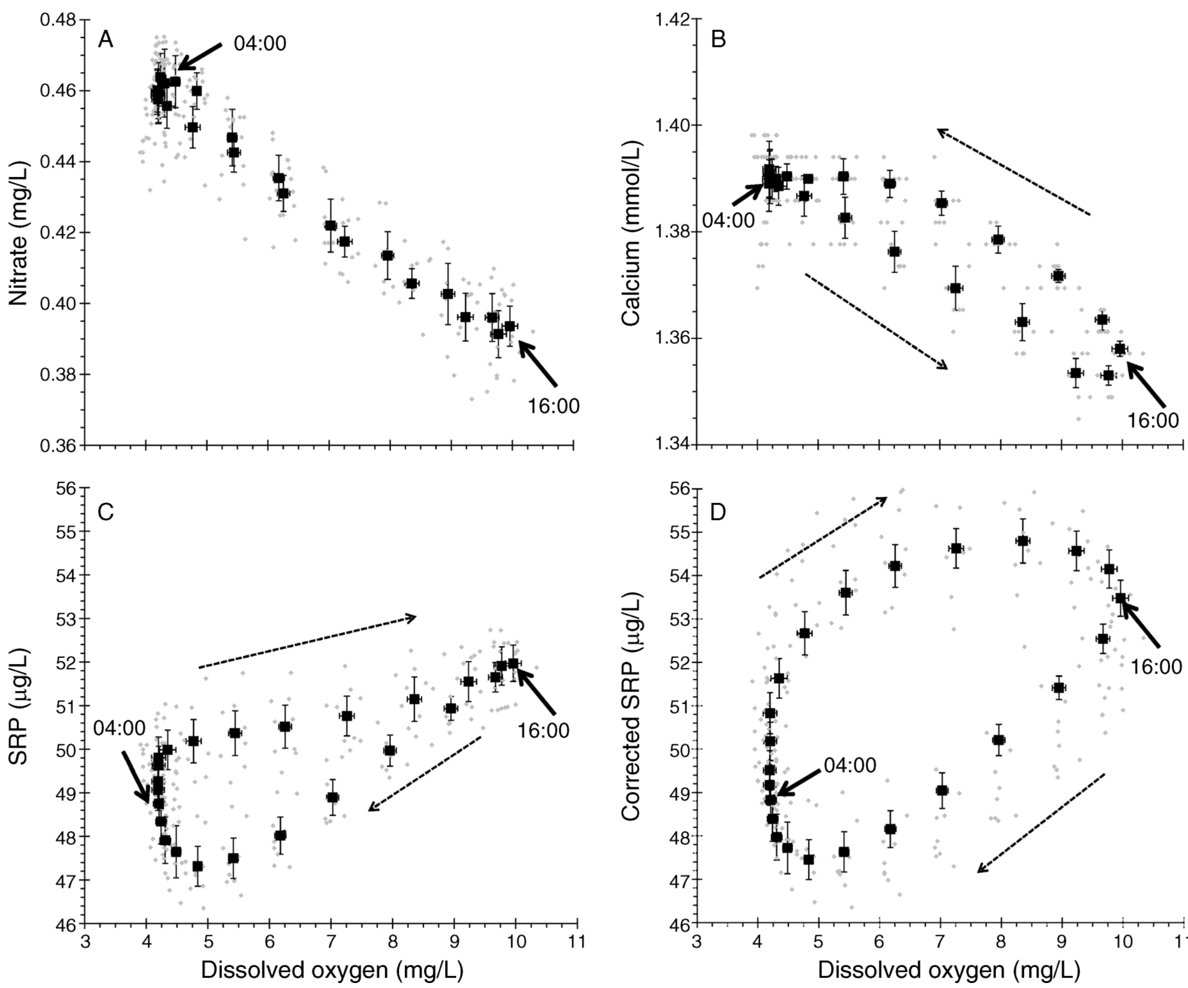

FIG. 6. Short time-scale covariation between dissolved oxygen (DO) and other solutes for March 2011 showing (A) [NO_3], (B) imputed [Ca], and both (C) raw and (D) corrected [SRP]. DO variation lags [Ca] (~1–2 hours) and leads SRP (~8 hours). Black squares indicate hourly means (± SD) over the deployment; gray circles are the raw data. Different lag geometry between panels C and D arise due to out-of-phase effects of calcite co-precipitation on SRP concentrations, which are adjusted for in panel D.

TABLE 3. Summary of metabolism and nutrient assimilation by deployment.

	Metabolic rates ($g\ O_2 \cdot m^{-2} \cdot d^{-1}$)		SRP assimilation (μg P/ L)		Benthic uptake rate, U ($mg\ N \cdot m^{-2} \cdot d^{-1}$)				
Deployment	GPP	ER	$SRP_{m,R}$	$SRP_{m,C}$	$U_{a,N}$	$U_{d,N}$	$U_{a,R,P}$	$U_{a,C,P}$	$U_{c,C,P}$
2009									
Sep	9.5 ± 0.7	−9.3 ± 0.1	54.7 ± 0.6	57.1 ± 1.6	95.1 ± 6.9	775.7 ± 24.8	8.3 ± 2.4	12.1 ± 2.4	5.8 ± 0.8
2010									
Apr†	15.9 ± 0.8	−12.8 ± 0.2	47.8 ± 0.8	50.8 ± 1.1			7.9 ± 1.6	16.2 ± 1.8	5.4 ± 1.6
May	18 ± 1	−13.5 ± 0.1	44 ± 0.4	48.2 ± 0.6	172.6 ± 28.1	1010.7 ± 99.6	8.9 ± 1.4	20.9 ± 2.3	7.8 ± 2.3
Oct	9.2 ± 0.3	−10 ± 0	49.2 ± 0.6	51.4 ± 0.9	73.1 ± 14.4	698 ± 16.2	3 ± 0.4	8.7 ± 0.5	3.5 ± 0.5
Dec	6.6 ± 0.8	−9.1 ± 0.4	60.4 ± 0.7	62.2 ± 0.7	57.3 ± 13.2	508.4 ± 24.4	1.8 ± 0.9	6.4 ± 1.5	2.7 ± 0.8
2011									
Feb	6.5 ± 1.8	−8.1 ± 0.3	57.1 ± 1.5	59.7 ± 1.6	56 ± 23.2	517.5 ± 51.1	6.3 ± 2.6	7.5 ± 5.1	4.5 ± 1.7
Mar	13.8 ± 0.2	−10.2 ± 0.1	51.5 ± 0.6	54.6 ± 1	123.1 ± 4.6	714.5 ± 28.5	8.5 ± 1	16.5 ± 2	5.1 ± 1
May	14.8 ± 1.9	−11 ± 0.1	53.2 ± 1.9	56.4 ± 1.7	158.8 ± 35.3	633.9 ± 72.6	11.3 ± 4.4	19.6 ± 3.4	8.0 ± 1.5

Notes: Values are means ± SD. Included are gross primary production (GPP), ecosystem respiration (ER), autotrophic assimilation of N ($U_{a,N}$), denitrification ($U_{d,N}$), daily SRP concentration maxima for both raw ($SRP_{m,R}$) and calcite co-precipitation corrected ($SRP_{m,C}$) data, autotrophic P assimilation for both baselines ($U_{a,R,P}$ and $U_{a,C,P}$), and estimated P mass loss to calcite co-precipitation ($U_{c,C}$).

† SUNA failed during April 2010 deployment; no N removal rates were estimated.

to NPP, we obtained a mean C:P ratio from raw concentrations of 945:1 vs. 466:1 for calcite-adjusted concentrations. Estimates of system-scale autotroph stoichiometry (including C:N and N:P as well) on a molar basis were relatively constant across deployments (Fig. 9). There was some evidence of a declining trend with GPP as predicted, but this was statistically significant for C:P only. Comparing mean C:P and C:N in spring (during maximum algal production) and fall yielded a significant difference for C:P only (476 ± 32 vs. 437 ± 24 [mean ± SD] for fall and spring, respectively; $P = 0.04$). Given that inferred autotroph stoichiometry varied little across deployments, we pooled all daily estimates for comparison with measured tissue stoichiometry (Fig. 10). Notably, ecosystem C:P ratio (466 ± 12) was slightly below the measured C:P of vascular plant taxa (478 ± 21) and higher than that of algal taxa (431 ± 24). In contrast, inferred C:N at the system scale was higher than both algal and vascular plant measurements, and N:P slightly lower than both. We note, however, that the comparison in Fig. 10 reports error estimates of ecosystem stoichiometry only from temporal variation, not due to the underlying parameter assumptions, particularly for estimating co-precipitation fluxes, that would expand considerably the uncertainty bounds.

DISCUSSION

This study documents coherent diel SRP variation in flowing waters, behavior consistent with patterns observed for other solutes (Odum 1956, Roberts and Mulholland 2007, Heffernan and Cohen 2010, Rusjan and Mikos 2010, Nimick et al. 2011), but rarely observed. In the basic waters of the Ichetucknee River,

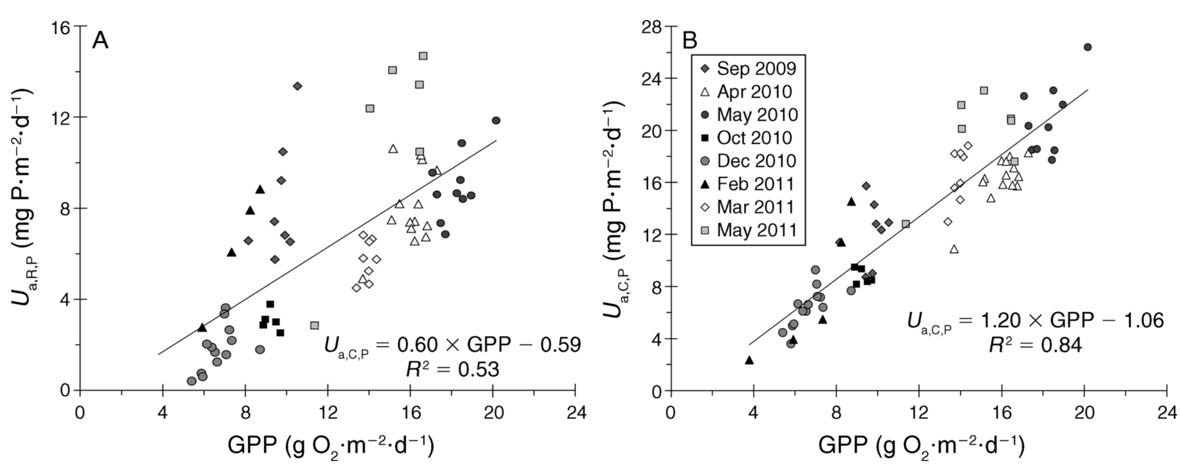

FIG. 7. Covariance between estimated P assimilation and gross primary production (GPP) across the eight deployments for (A) $U_{a,R,P}$ and (B) $U_{a,C,P}$. The resulting mean molar C:P ratio of ecosystem metabolism is high (945:1) for the former, but reasonable (455:1) for the corrected data.

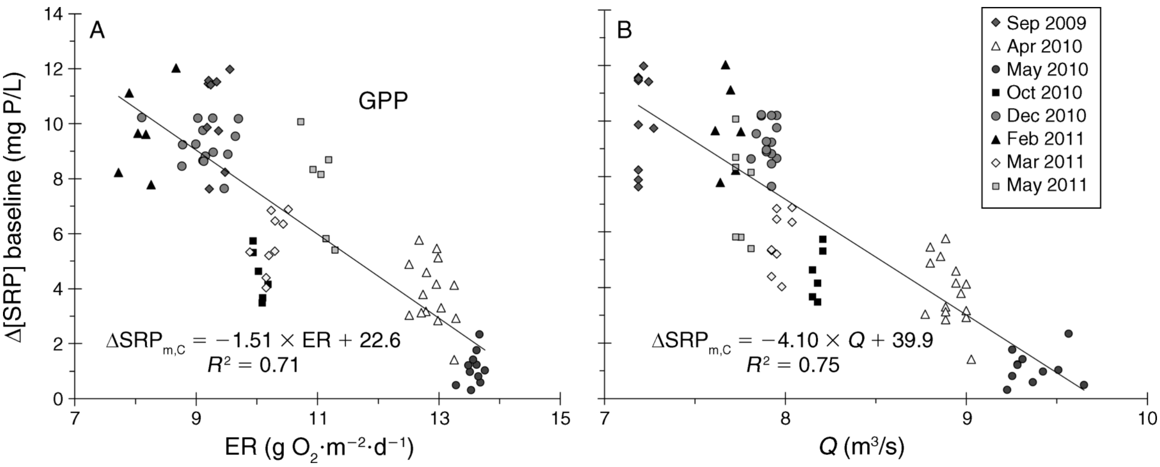

FIG. 8. The diel SRP baseline is adjusted upward following correction for calcite co-precipitation. The magnitude of that upward adjustment is strongly correlated with (A) ecosystem respiration (ER) and (B) flow (Q) and is relatively consistent within deployments.

this diel SRP signal was temporally asymmetrical, which was best explained as the result of two overlapping processes, one due to autotrophic assimilation and another due to co-precipitation with calcite, both of which are mediated by ecosystem metabolism. The importance of both retention pathways lends strong support to our central hypothesis that stoichiometry at the ecosystem level arises from direct and indirect coupling of biogeochemical processes with ecosystem energetics (Sterner and Elser 2002, Schade et al. 2005, Fellows et al. 2006). The ability to disentangle these signals illustrates the emerging utility of in situ measurements for testing hypotheses about the coupled dynamics of ecosystem processes.

Sensors for inferring process

In situ sensors capable of measurements of solute chemistry in real time, and without the potential confounding errors created by sampling and holding-time effects, enable novel analyses of coupled biogeochemical cycles. Our results illustrate the value of monitoring a broad suite of solutes, which can be used to disentangle complex temporal dynamics and interactions among metabolic, hydrologic, and geochemical processes (Kirchner et al. 2004). Expanding the basic approach developed here to other systems with more dynamic hydrologic inputs, different geochemical processes, and larger importance of heterotrophic demand may require more complex analyses than those presented. Despite these potential challenges, passive observation of fine-scale nutrient concentrations complements existing approaches in several ways. First, in situ nutrient sensors capture temporal dynamics, such as lags in P assimilation observed here, or short-term GPP effects on denitrification (Heffernan and Cohen 2010), that conventional measurement approaches cannot reasonably resolve. The literature is replete with examples of solute variation occurring at diel (e.g., Liu et al. 2008, Rusjan and Mikos 2010), event (Holloway and Dahlgren 2001), and seasonal time scales (Pellerin et al. 2012), and patterns of solute variation with discharge are increasingly viewed as diagnostic of watershed condition (Basu et al. 2010). High-frequency measurements from in situ sensors offer unique promise for

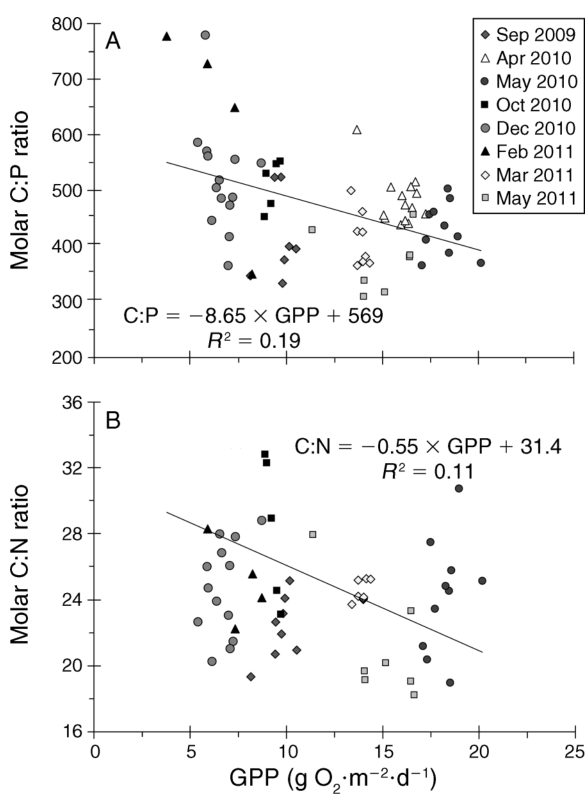

FIG. 9. Increasing GPP across the eight deployments leads to significant lower system-scale C:P stoichiometry (A; P = 0.02). A similar trend for C:N was not significant (B; P = 0.12).

better understanding these dynamics and drawing new inference about the processes that create them.

Second, the deployment of nutrient sensors is not constrained by the myriad technical challenges of manipulating the chemistry of larger water bodies (e.g., using enrichment dosing [Tank et al. 2008, Covino et al. 2010]), and so can be used in larger rivers (and potentially lakes) where solute releases are logistically untenable. This may allow methodologically consistent scale-independent measurements of riverine nutrient processing, which remains an open question pertinent to network-scale nutrient management (Alexander 2000, Wollheim et al. 2006).

Finally, use of in situ sensors obviates many sample collection and processing steps, each of which accumulate error that may mask relatively subtle signals. In-line analysis eliminates the need for washed sample containers (by sampling and filtering directly into the autoanalyzer), dramatically reduces holding times (<1 hour), and retains samples at ambient temperature throughout the analysis. In this case, the diel signal is clear even with as little as 3 μg P/L diel variation (Fig. 5), an amplitude difficult to resolve in typical laboratory analyses.

Geochemical and assimilatory P retention

While numerous studies have shown diel variation in soluble nitrogen (Vincent and Downes 1980, Triska et al. 1989, Harrison et al. 2005, Roberts and Mulholland 2007, Heffernan and Cohen 2010, Rusjan and Mikos 2010) as well as a suite of other solutes (McKnight and Bencala 1988, de Montety et al. 2011, Nimick et al. 2011, Fortner 2012), very few have observed diel SRP variation (e.g., Vincent and Downes 1980, Gammons et al. 2011). Indeed, several studies explicitly report the absence of consistent P variation in spite of consistent diel periodicity in other nutrients (Triska et al. 1989, Kuwabara 1992, Hatch et al. 1999, Parker et al. 2007). The absence of observed diel variation may arise because the magnitude of the variation in less productive systems may be too small to resolve, a problem partially alleviated by the methodological advantages of in situ sensors. The absence of reported diel P dynamics could also occur if the influence of geochemical reactions were larger or in response to a wider array of reactions. Diurnal variation in P reactions may occur in response to insolation (e.g., photoreduction of Fe in acid streams [McKnight and Bencala 1988]); varying redox conditions (Kim et al. 2003); indirect effects of primary production (e.g., mineral precipitation leading to co-precipitation [House and Plant 2002, Nimick et al. 2011]); and even snowmelt- or transpiration-driven variation in flow (Fortner et al. 2012). Our results indicate approximately equal but out of phase assimilatory (66%) and geochemical/co-precipitation (34%) fluxes. In less productive aquatic ecosystems, diurnal P variation due to assimilation may be masked by these countervailing geochemical and hydrologic processes.

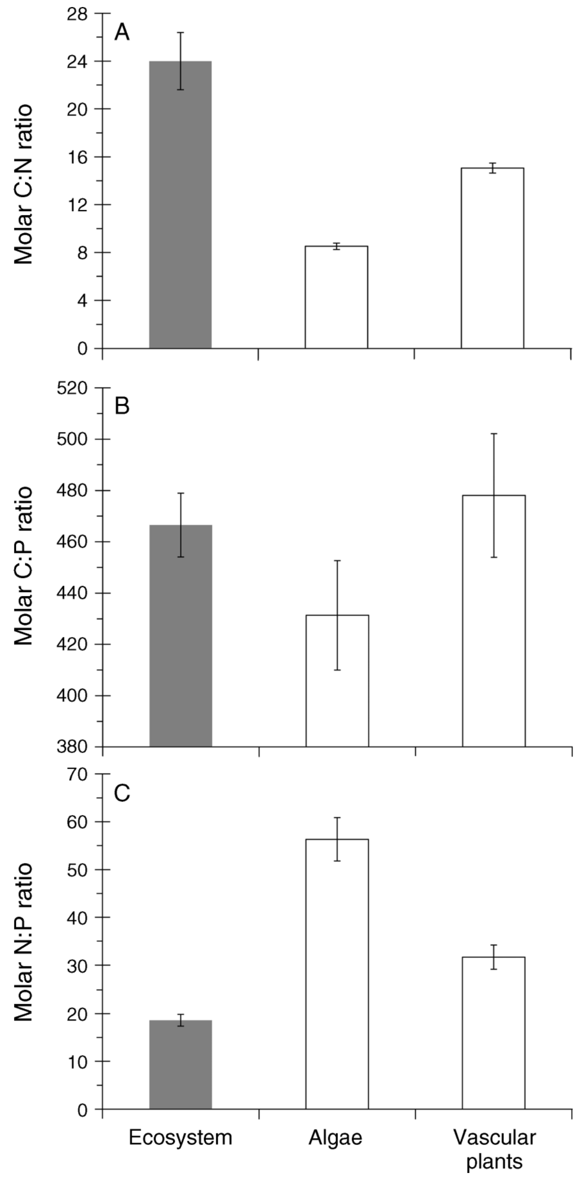

FIG. 10. Comparison between inferred ecosystem molar stoichiometry (gray bars) and measured tissue stoichiometry (white bars) of the dominant autotrophs in the Ichetucknee River for (A) C:N, (B) C:P, and (C) N:P. Error bars denote 95% confidence intervals over time (for daily estimates of ecosystem stoichiometry) and across replicate samples (for tissue stoichiometry).

In the special case of the Ichetucknee River, which is, like all study systems, unique in the relative importance of the myriad reaction pathways, the array of potential geochemical retention pathways except for calcite co-precipitation could be reasonably ruled out based on several lines of evidence. First, other P-binding carbonate minerals ($MgCa(CO_3)_2$, dolomite; $MgCO_3$, magnesite; $FeCO_3$, siderite; $MnCO_3$, rhodochrosite; and $BaCO_3$, witherite) are always undersaturated in the river (M. J. Kurz, V. de Montety, J. B. Martin, M. J. Cohen, and C. R. Foster, *unpublished manuscript*), which argues against the importance of associated co-precipitation pathways. Second, while a variety of metals exhibit diel variation in the Ichetucknee, including Ba, Fe, Cu, U, Mn, and Sr, only Fe variation was in-phase with diel SRP variation. The amplitude of all diel metal concentration signals was too small to account for a relevant fraction of observed SRP variation based on the stoichiometry of phosphate mineral formation. Iron exhibits the largest diel amplitude of all the metals measured in the Ichetucknee River (~2 μg/L; M. J. Kurz, V. de Montety, J. B. Martin, M. J. Cohen, and C. R. Foster, *unpublished manuscript*). If observed Fe variation were due entirely to ferric-phosphate mineral formation, which is unlikely, and this mineral was entirely solubilized during the day via photoreduction (McKnight and Bencala 1988), also unlikely in this alkaline setting, the variation in Fe concentrations would explain less than 10% of observed SRP signal. In contrast, the Ichetucknee River is always slightly over-saturated with respect to calcite (de Montety et al. 2011), particularly so during the day in response to photosynthesis, suggesting a net precipitation flux. Moreover, the amplitude of diel [Ca] variation is commensurate with observed variation in SRP, suggesting that calcite co-precipitation figures prominently in the SRP signal. The dominant processes in other rivers will undoubtedly be different in relative magnitude, and may also include processes that could reasonably be neglected here (Fig. 1B).

Extracting the effects of calcite co-precipitation to isolate the autotrophic uptake signal required several important assumptions. While reaction rates are relatively well understood, several parameters that govern the magnitude of mass flux are uncertain. Three of these merit explicit attention. First is the assumption that specific conductance is a reasonable proxy for [Ca] in water with a complex ionic mixture and numerous diel cycles (e.g., nitrate). Strong positive covariance between Ca and SpC with relatively consistent slopes across autosampler deployments (Fig. 3) suggests the association is robust. While this assumption is difficult to validate explicitly, we note that the resulting P co-precipitation fluxes are relatively insensitive to observed slope variation. Changing the SpC vs. [Ca] slope from 0.041 to 0.043 $\mathrm{mmol \cdot L^{-1} \cdot cm^{-1} \cdot \mu S^{-1}}$ (mean vs. maximum value) changes the resulting inference of benthic P assimilation less than 5% (e.g., mean $U_{a,C,P} = 20.9$ vs. 21.6 mg $\mathrm{P \cdot m^{-2} \cdot d^{-1}}$, respectively, for May 2010). More influential is the second assumption regarding the value of the surface density of co-precipitated P (σ in Eq. 2). Laboratory values in relatively simple solutions typically fall between 0.12 to 0.27 μmol/m^2. However, field estimates of this parameter are much lower (~0.055 μmol/m^2 [House 1990]). One explanation for lower value observed under field conditions is the suite of other co-precipitation reactions that may serve to reduce the effective calcite area for P sorption. While we ultimately adopted a low published value for a chalk stream, the potential error associated with this is large. Changing σ to a value commonly estimated in laboratory studies of 0.15 μmol/m^2 increases the co-precipitation flux from 20.9 to 42.8 mg $\mathrm{P \cdot m^{-2} \cdot d^{-1}}$ (for May 2010), significantly weakens the association of $U_{a,C,P}$ with GPP, and renders the resulting C:P ratios implausibly low (C:P = 210:1). Finally, we observed a significant (~2 hour) lag between [Ca] and changes in SpC, which was replicated across all autosampler deployments. The mechanism for this lag is unknown, but may arise from impacts on SpC of other ions (e.g., NO_3, Mg) whose cycling occurs slightly to substantially out of phase with Ca.

Timing of assimilatory P retention

Recognizing and controlling for co-precipitation fluxes in the raw data isolates a diel SRP signal that is far more symmetric with DO (Fig. 6C vs. 6D); this adjusted signal was interpreted as P assimilation. The most surprising aspect of this signal is the substantial lag (~8 hours) between peak primary production and P assimilation; no such lag was observed between C and N assimilation (Heffernan and Cohen 2010, de Montety et al. 2011). While this is the first study that we are aware of that consistently and quantitatively demonstrates this lag, other studies tentatively support the generality of substantial SRP cycle lags behind other solutes such as nitrate (Vincent and Downes 1980, Gammons et al. 2011). In some cases, this geometry of the SRP signal is strikingly similar to the 8 hour lag pattern observed here. For example, Grimm et al. (1981) observed weak diel P variation in a Sonoran Desert stream that was out-of-phase with expectations of synchronized uptake of mineral P and C. Notably, diel removal peaks occurred at night and were bi-modal, potentially indicating geochemical interactions early in the day. Kimura et al. (1999) report that an estuarine alga assimilated P at night during diel migrations out of the photic zone, and used that P during the day. While this may be a special case induced by spatial variation in P availability, it does suggest some plasticity in organismal uptake timing. More recent results from experimental stream-side channels suggest seasonally consistent and statistically significant decreases in stream water SRP at night (Matheson et al. 2012), consistent with the signals observed in this work. At a smaller scale, Ahn et al. (2002) observed strong diel P removal variation across three algal taxa in controlled laboratory cyclostats. Diel patterns varied across taxa, but generally lagged 6–10 hours behind peak instantaneous growth rates.

Despite some precedent for the signals we observed, not all literature supports the plausibility or generality of a P uptake lag. For example, Beck and Bruland (2000) observed synchronized depletion of NO_3 and SRP in a shallow productive estuary. In a broad review of algal nutrient assimilation, Healey (1973) reports that light actually stimulates P uptake, albeit only at very high concentrations (i.e., no effect below 300 μg P/L) and with significant variation in timing that appears related to taxa-specific variation in cell division. As such, it may be that P variation in lotic systems at lower concentrations is controlled by the diurnal timing of organism cell-division (Kalita et al. 2007), with demand controlled by P requirements for ribosomal RNA production (Sterner and Elser 2002, Elser et al. 2003). RNA mass and rRNA/DNA ratios in aquatic animals (Chicharo et al. 2001) and algal tissues (Lepp and Schmidt 1998) exhibit strong diel periodicity with peak levels at night, which is consistent with patterns observed here. Further research is needed to elucidate mechanisms and generality of this lagged uptake effect, but if this diel rRNA hypothesis is correct, it represents a novel, temporally dynamic link between organismal physiology and whole-ecosystem nutrient fluxes.

The assumption that SRP variation after adjusting for co-precipitation due to assimilation (i.e., $U_{a,C,P}$) is supported principally by correlative evidence; namely, that P uptake is well predicted by primary production (Fig. 7B). That direct link with metabolism was further illustrated by the observation that insolation variation led to clear changes in diel SRP amplitude in all but two deployments. For example, on 19 December 2010 (Fig. 5), cloud cover led to lower than typical irradiance (719 $W \cdot m^{-2} \cdot d^{-1}$), and thus lower diel DO variation. On that day we observed a dramatic decline in the diel SRP signal. This variation in cloud cover led to strong within-deployment covariance between GPP and $U_{a,C,P}$ (r = 0.73, P = 0.006). While this did not hold for all deployments (note within deployment covariance in Fig. 7B), the most likely explanation is that we observed minimal variation in insolation within most deployments.

Baseline variation and reach-scale mass balance

The co-precipitation flux is highest during the day. This coincides with the time of day when the daily baseline concentration, SRP_m, is set. Estimates of P assimilation are strongly influenced by both day-to-day variation and co-precipitation adjustments to this quantity because it sets the upper-bound against which measured SRP variation is compared. As such, the embedded assumptions in arriving at this number are of critical importance. These include (1) assimilation at SRP_m is negligible, (2) SRP_m changes evenly from one day's baseline to the next, and (3) day-to-day variation in the baseline is possible. Two lines of evidence support the first assumption. First, we observed strong correlation between GPP and $U_{a,C,P}$ whose slope yields plausible estimates of elemental uptake ratios. Relaxing the assumption to allow nighttime uptake would degrade both the fit and stoichiometry of the GPP vs. $U_{a,C,P}$ relationship. Second, because the river gains P between the springs and downstream station (Figs. 4 and 5; dashed input line below measured concentrations), allowing non-zero assimilation at SRPm would compound mass balance gaps. We also note this assumption was judged tenable when made for NO_3 assimilation (Heffernan and Cohen 2010). In that study, the additional possibility that the assimilatory signal is dispersed over a period exceeding 24 hours, which would violate this assumption for hydraulic reasons, was rejected because of short residence time (~6 hours [Hensley and Cohen 2012]). While P uptake clearly has important differences from N, the coherence of the diel cycle does suggest high temporal specificity of removal.

With respect to the second assumption, Heffernan and Cohen (2010) report improved model fit for N uptake using a baseline that is extrapolated from the preceding night rather than interpolated between two adjacent nights. Rapid baseline changes implied by this were linked to labile carbon controls on denitrification, but no comparable heterotrophic mechanism operates on P. Consequently, the extrapolated method, which also yielded a poorer fit vs. GPP, was not adopted and baseline variation was assumed to be linear between diel maxima.

Finally, the third assumption is that day-to-day variation in SRP_m is possible. One line of supportive evidence is that assuming constant SRP_m within a deployment substantially degrades the fit with GPP. Further correlative evidence comes from the observation that flow and ecosystem respiration both appear to successfully predict variation in SRPm (which we index to flow-weighted inputs to yield ΔSRP_m). Strong correlation between these variables complicates separation of their individual effects, but we note that both are negative, suggesting larger deviation from spring inputs at low flow and low ER. Redox controls may be important due, for example, to higher solubility of Fe^{2+} than Fe^{3+}, with consequences for the effects of diel DO variation and impacts of ecosystem respiration on the SRP baseline. The predictive power of both flow and ER primarily reflect variation among rather than within deployments. Controls remain unresolved for day-to-day variation in SRP_m within deployments.

P fluxes out the Ichetucknee River study reach cannot be explained by measured spring vent inputs (Table 1). The magnitude of this P mass deficit is actually magnified by correction for calcite co-precipitation, which increases the SRPm (Fig. 4, Table 3). This additional P source is temporally variable across deployments (Figs. 4 and 5), and may arise from several sources. One possibility is that internal ecosystem P stores are not in long-term equilibrium, and the reach-scale P gain is derived from the transient depletion of internal pools (e.g., desorption, stored OM mineralization). Meyer and Likens (1979) and Jarvie et al. (2002) both argue that reach-scale mass balance varies with flow (net sink at low flow, net source at high flow). However, remarkably low flow variation, and the absence of scouring floods in this system, make this explanation unlikely. Short term variation in the ratio of mineralization to uptake is also unsupported, both by the relatively constant GPP : ER ratio (1.10 ± 0.27) and by the nearly constant temperatures that persist in this system year-round. As such, most of the variation in GPP : R is driven by day-to-day changes in GPP induced by cloud cover rather than seasonal differences, which are inconsistent with sustained source dynamics over each deployment. Invoking transient depletion of internal stores was ultimately rejected principally because we observed additional P delivery to the river in all deployments covering all seasons.

A more likely source of additional P is diffuse seepage of water. While there are six gaged springs, we have observed dozens of minor springs and seeps along the river. Potentiometric measurements in both the upper and lower river suggest a net gaining gradient (M. J. Kurz, J. B. Martin, and M. J. Cohen, *unpublished manuscript*), which supports the possibility of a combination of ungaged discrete inputs and diffuse inputs. In support of a relevant mass flux from ungaged sources, de Montety et al. (2011) estimate, based on chloride mass balance, that ~0.75 m^3/s of water similar in chemistry to the Mill Pond spring must be entering the river. Porewater sampling in the unconsolidated sediments of the river channel near Mill Pond spring suggests high SRP concentrations (~150 μg P/L [M. J. Kurz, J. B. Martin, and M. J. Cohen, *unpublished manuscript*]). Notably, these measurements also suggest negligible nitrate concentrations, so that previous reach-scale mass balances for N (Heffernan et al. 2010*a*, Heffernan and Cohen 2010) did not detect a similar deficit. Assuming constant porewater [SRP], we calculated the diffuse seepage flux (m^3/s) necessary to close the daily P mass balance, estimated as the difference between mass inputs from the springs and mass output that would have occurred without removal (i.e., using $SRP_m \times Q$). The imputed water flow was between 0.03 and 0.61 m^3/s, which is qualitatively consistent with previous estimates of diffuse water inputs (de Montety et al. 2011). In addition, the estimated diffuse seepage flux is strongly correlated with measured river discharge ($r = -0.90$, $P < 0.001$), suggesting that high river flows inhibit delivery of diffuse seepage, likely by reducing the head gradient between the river and groundwater.

Ecosystem stoichiometry

The application of stoichiometric theory to whole ecosystems requires an understanding of the elemental composition of individual organisms, their chemical environment, and the physical and biological processes that mediate exchanges between and among them (Schade et al. 2005). Previous studies of whole-stream N and P demand (Davis and Minshall 1999, Schade et al. 2011), which have demonstrated the link between organismal stoichiometry and whole ecosystem nutrient fluxes, are among the few examples of simultaneous, direct measurement of N and P assimilation at whole ecosystem scales. Our approach, based on inference of autotroph assimilation from diel variation in inorganic N and P, enables examination of stoichiometric relationships across multiple temporal scales, ranging from hours to seasons, and potentially beyond. In the Ichetucknee River, comparison between organismal and ecosystem stoichiometry provides theoretical validation of our approach, but also raises new questions about the link between the elemental composition of organisms and whole-system nutrient demand.

Stoichiometric theory suggests that autotrophic elemental ratios are influenced by the ratio of light and nutrient availability (Sterner and Elser 2002), a pattern that is often (Klausmeier et al. 2004) but not always (Hall et al. 2005) supported empirically. We observed a modest correlation between C:P of ecosystem assimilation and GPP (Fig. 9A), and no significant relationship for C:N (Fig. 9B). This latter observation contrasts somewhat with previous observations of mid-day shifts toward lower C:N ratios during periods of high productivity (Heffernan and Cohen 2010). Overall, however, relative homeostasis in response to varying light: nutrient ratios suggests nutrients are not limiting in this enriched, chemostatic ecosystem (Sterner and Elser 2002). This inference is consistent with other studies that have identified light as the resource limiting ecosystem metabolism (Odum 1957, Heffernan et al. 2010*b*).

One potential application of repeated measures of the stoichiometry of ecosystem N and P assimilation is to partition productivity and nutrient demand among complex mixtures of autotrophs. While our efforts are preliminary, our results support the conclusion that vascular plants, which dominate the benthic surface in this river, also dominate primary production. Specifically, the C:P ratio of ecosystem metabolism (466:1) is closer to vascular plant tissues (478:1) than filamentous algae that proliferate in some of the spring vents and slack-water areas (431:1). These ratios fall within previously reported values for marine plants (interquartile range ~400:1 to 700:1 [Atkinson and Smith 1983]). It is unclear whether moderate shifts in C:P with increased productivity (Fig. 9A) reflect shifts in tissue stoichiometry within taxa or changes in the relative contribution of algae and vascular plants to ecosystem primary productivity.

In contrast to C:P ratios, ecosystem C:N (~24:1) and N:P (~18:1) were markedly higher than tissue measurements for either vascular or algal autotrophs. Several explanations for this are possible. This result may reflect underestimation of $U_{a,N}$, which could plausibly occur for several reasons. For example, violating the assumption of diurnally constant denitrification, as isotopic evidence from this system tangentially suggests (Cohen et al. 2012), would presumably create nitrate variation out of phase with assimilation (i.e., DO inhibition of denitrification when assimilation is largest), leading to systematic underestimation of $U_{a,N}$. Alternatively, extracellular exudates may be an important repository of carbon fixed during gross primary production but are particularly N poor (e.g., enzymes or extracellular polysaccharides). As such, measured tissue stoichiometry may not accurately reflect ecosystem-scale metabolic allocations.

The mismatch might also derive from decisions about which tissues were sampled. Other studies in these systems report higher C:N ratios for vascular plant tissues (e.g., 25:1 in Duarte and Canfield [1990]), and a broader analysis of rooted marine vascular plants, which are evolutionary relatives of taxa sampled here, also suggested higher values (mean, 22:1; range, 10:1 to 50:1 [Atkinson and Smith 1983]). While we are confident our measurements are accurate since they have subsequently been replicated (R. L. Douglass, *unpublished data*), we did intentionally selected new growing tips (and no roots) to reduce confounding effects of attached algae and detrital matter. These new shoots may have lower C:N ratios than mature leaves, limiting the generality of our estimates (~15:1) for combined vascular plant metabolism at the ecosystem scale. The relative partitioning of assimilated C and N to different tissues, and with leaf aging, merit investigation to understand the observed stoichiometric mismatch.

The precision of estimated stoichiometry of ecosystem assimilation from diel nutrient variation, and inferences that can be drawn from them, depend on three principal assumptions that merit further investigation. First, inference of geochemical P removal is predicated on models of co-precipitation of P with calcite that have not been validated in the Ichetucknee. Since estimates of calcite surface area (σ) and the timing of co-precipitation flux both strongly influence $SRP_{m,C}$ and thus the inferred magnitude of uptake, field measurements of these geochemical interactions would improve the precision and confidence of these estimates.

Another important assumption that influences inferred ecosystem stoichiometry is that denitrification is diurnally constant, which attributes the entirety of diel nitrate variation to assimilation (Heffernan and Cohen 2010). There is evidence in the Ichetucknee (Cohen et al. 2012) and other systems (Christensen et al. 1990, Laursen and Seitzinger 2004, Harrison et al. 2005) that denitrification is time varying in response to oxygen availability, although the magnitude of this variation remains unresolved. The primary consequence of reduced denitrification during the day would be underestimation of inferred autotrophic removal. This could explain why comparisons between measured tissue stoichiometry and ecosystem stoichiometry for both C:N and N:P suggest that our estimates of $U_{a,N}$ may be too small.

Finally, our comparison of autotroph tissue stoichiometry and ecosystem assimilation assumes that all assimilated nutrients (including C) are incorporated into biomass. Aquatic plants, including algae and other microbial primary producers, are notoriously leaky, losing large quantities of assimilated nutrients to the environment (Khailov and Burlakova 1969, Larsson and Hagstrom 1979, Descy et al. 2002, Webster et al. 2005). If material exuded by primary producers in the Ichetucknee River differs in elemental composition from standing biomass, as has been observed in other systems (e.g., transparent exopolymers with high C:N; Passow 2002), then our expectation that ecosystem and organismal stoichiometry will match is invalid. Understanding the stoichiometry of exudation may prove essential to reconciling elemental composition of vegetation and whole-ecosystem assimilation.

Conclusions

Biogeochemical cycles are coupled by numerous biotic and abiotic processes, with important implications for ecosystem dynamics at scales from local to global (Aufdenkampe et al. 2011, Burgin et al. 2011). Despite widespread attention to these interactions, relatively little work has been done on the time scales over which different mechanisms link major element cycles (Finzi et al. 2011). Our results illustrate the complex temporal dynamics that arise from interactions among metabolic and geochemical processes, even in a relatively homeostatic ecosystem. High-frequency measurements of water chemistry provide a novel way to observe these couplings, and to develop and test theory about the timescales of coupled biogeochemical cycles. In this case, we were able to separate direct and indirect metabolic controls on P dynamics, and quantify the stoichiometry of ecosystem primary production.

The widespread success of stoichiometric theory to predict behaviors of organelles, organisms, and food webs means that tools for assessing elemental coupling across scales will remain crucial for understanding pattern and process in ecological systems. The recent emergence of passive sensor-based approaches for evaluating elemental coupling at the ecosystem level, in our case using rivers as model systems, appears to be a promising way to test the generality of stoichiometric theory, and to explore the complex reciprocal interactions between organisms and their environment. The origins of metabolism estimates in flowing waters are in high temporal resolution measurements of dissolved oxygen (Odum 1956); our effort to extend this fundamental logic to other critical solutes, thereby revealing both their individual cycles but also their coupling, promises a new array of ecological insights.

Acknowledgments

We thank Larry Kohrnak for help with sampling logistics, and Ginger Morgan at Ichetucknee Springs State Park and the staff at the Florida Department of Environmental Protection for assistance with site access and sensor protection. This research was supported by grants from the St. Johns River Water Management District (SJ#25140) and the National Science Foundation (EAR #0838369 and #0853956). M. J. Cohen conceived of the study, performed research, analyzed data, contributed new methods, and wrote the paper; M. J. Kurz performed research, analyzed data, and contributed new methods; J. B. Heffernan conceived of the study, contributed new methods, and wrote the paper; J. B. Martin conceived of the study, contributed new methods, and wrote the paper; R. L. Douglass performed research; C. R. Foster performed research; and R. G. Thomas contributed new methods.

Literature Cited

Ahn, C. Y., A. S. Chung, and H. M. Oh. 2002. Diel rhythm of algal phosphate uptake rates in P-limited cyclostats and simulation of its effect on growth and competition. Journal of Phycology 38:695–704.

Alexander, R. B., R. A. Smith, and G. E. Schwarz. 2000. Effect of stream channel size on the delivery of nitrogen to the Gulf of Mexico. Nature 403:758–761.

Arango, C. P., J. L. Tank, L. T. Johnson, and S. K. Hamilton. 2008. Assimilatory uptake rather than nitrification and denitrification determines nitrogen removal patterns in streams of varying land use. Limnology and Oceanography 53:2558–2572.

Atkinson, M. J., and S. V. Smith. 1983. C:N:P ratios of benthic marine plants. Limnology and Oceanography 28:568–574.

Aufdenkampe, A. K., E. Mayorga, P. A. Raymond, J. M. Melack, S. C. Doney, S. R. Alin, R. E. Aalto, and K. Yoo. 2011. Riverine coupling of biogeochemical cycles between land, oceans, and atmosphere. Frontiers in Ecology and the Environment 9:53–60.

Basu, N. B., et al. 2010. Nutrient loads exported from managed catchments reveal emergent biogeochemical stationarity. Geophysical Research Letters 37:L23404.

Beck, N. G., and K. W. Bruland. 2000. Diel biogeochemical cycling in a hyperventilating shallow estuarine environment. Estuaries 23:177–187.

Bennett, E. M., S. R. Carpenter, and N. F. Caraco. 2001. Human impact on erodible phosphorus and eutrophication: a global perspective. BioScience 51:227–234.

Burgin, A. J., W. H. Yang, S. K. Hamilton, and W. L. Silver. 2011. Beyond carbon and nitrogen: how the microbial energy economy couples elemental cycles in diverse ecosystems. Frontiers in Ecological and the Environment 9:44–52.

Chapin, T. P., J. M. Caffrey, H. W. Jannasch, L. J. Colletti, J. C. Haskins, and K. S. Johnson. 2004. Nitrate sources and sinks in Elkhorn Slough, California: results from long-term continuous in situ nitrate analyzers. Estuaries and Coasts 27:882–894.

Chicharo, L. M. Z., M. A. Chicharo, F. Alves, A. Amaral, A. Pereira, and J. Regala. 2001. Diel variation of the RNA/DNA ratios in *Crassostrea angulate* (Lamarck) and *Ruditapes decussatus* (Linnaeus 1758) (Mollusca: Bivalvia). Journal of Experimental Marine Biology and Ecology 259:121–129.

Christensen, P. B., L. P. Nielsen, J. Sorensen, and N. P. Revsbach. 1990. Denitrification in nitrate-rich stream: diurnal and seasonal variation related to benthic oxygen metabolism. Limnology and Oceanography 35:640–651.

Cohen, M. J., J. B. Heffernan, A. Albertin, and J. B. Martin. 2012. Inference of riverine nitrogen processing from longitudinal and diel variation in dual nitrate isotopes. Journal of Geophysical Research—Biogeosciences 117:G01021.

Covino, T. P., B. L. McGlynn, and R. A. McNamara. 2010. Tracer additions for spiraling curve characterization (TASCC): quantifying stream nutrient uptake kinetics from ambient to saturation. Limnology and Oceanography 8:484–498.

Cross, W. F., J. P. Benstead, P. C. Frost, and S. A. Thomas. 2005. Ecological stoichiometry in freshwater benthic systems: recent progress and perspectives. Freshwater Biology 50:1895–1912.

Davis, J. C., and G. W. Minshall. 1999. Nitrogen and phosphorus uptake in two Idaho (USA) headwater wilderness streams. Oecologia 119:247–255.

de Montety, V., J. B. Martin, M. J. Cohen, C. Foster, and M. J. Kurz. 2011. Influence of diel biogeochemical cycles on carbonate equilibrium in a karst river. Chemical Geology 283:31–43.

Descy, J. P., B. Leporcq, L. Viroux, C. Francois, and P. Servais. 2002. Phytoplankton production, exudation and bacterial reassimilation in the River Meuse (Belgium). Journal of Plankton Research 24:161–166.

Diaz, O. A., K. R. Reddy, and P. A. Moore, Jr. 1994. Solubility of inorganic phosphorus in stream water as influence by pH and calcium concentration. Water Research 28:1755–1763.

Duarte, C. M., and D. E. Canfield. 1990. Macrophyte standing crop and primary production in some Florida spring-runs. Water Resources Bulletin 26:927–934.

Duarte, C. M., Y. T. Prairie, T. K. Frazer, M. V. Hoyer, S. K. Notestein, R. Martinez, A. Dorsett, and D. E. Canfield. 2010. Rapid accretion of dissolved organic carbon in the springs of Florida: the most organic-poor natural waters. Biogeosciences 7:4051–4057.

Elser, J. J., et al. 2003. Growth rate-stoichiometry couplings in diverse biota. Ecology Letters 6:936–943.

Elser, J. J., M. E. S. Bracken, E. E. Cleland, D. S. Gruner, W. S. Harpole, H. Hillebrand, J. T. Ngai, E. W. Seabloom, J. B. Shurin, and J. E. Smith. 2007. Global analysis of nitrogen and phosphorus limitation of primary producers in freshwater, marine and terrestrial ecosystems. Ecology Letters 10:1135–1142.

Elser, J. J., D. R. Dobberfuhl, N. A. MacKay, and J. H. Schampel. 1996. Organism size, life history, and N:P stoichiometry. BioScience 46:674–684.

Elser, J. J., R. W. Sterner, E. Gorokhova, W. F. Fagan, T. A. Markow, J. B. Cotner, J. F. Harrison, S. E. Hobbie, G. M. Odell, and L. J. Weider. 2000. Biological stoichiometry from genes to ecosystems. Ecology Letters 3:540–550.

Elser, J. J., and J. Urabe. 1999. The stoichiometry of consumer-driven nutrient recycling: theory, observations, and consequences. Ecology 80:735–751.

Fellows, C. S., H. M. Valett, C. N. Dahm, P. J. Mulholland, and S. A. Thomas. 2006. Coupling nutrient uptake and energy flow in headwater streams. Ecosystems 9:788–804.

Finzi, A. C., J. J. Cole, S. C. Doney, E. A. Holland, and R. B. Jackson. 2011. Research frontiers in the analysis of coupled biogeochemical cycles. Frontiers in Ecology and the Environment 9:74–80.

Fisher, S. G. 1997. Creativity, idea generation, and the functional morphology of streams. Journal of the North American Benthological Society 16:305–318.

Fortner, S. K., W. B. Lyons, and L. Munk. 2012. Diel stream geochemistry, Taylor Valley, Antarctica. Hydrological Processes. http://dx.doi.org/10.1002/hyp.9255

Frost, P. C., M. A. Evans-White, Z. V. Finkel, T. C. Jensen, and V. Matzek. 2005. Are you what you eat? Physiological constrains on organismal stoichiometry in an elementally imbalanced world. Oikos 109:18–28.

Galloway, J. N., et al. 2004. Nitrogen cycles: past, present and future. Biogeochemistry 70:153–226.

Gammons, C. H., J. N. Babcock, S. R. Parker, and S. R. Poulson. 2011. Diel cycling and stable isotopes of dissolved oxygen, dissolved inorganic carbon, and nitrogenous species in a stream receiving treated municipal sewage. Chemical Geology 283:44–55.

Grimm, N. B., S. G. Fisher, and W. L. Minckley. 1981. Nitrogen and phosphorus dynamics in hot desert streams of the Southwestern USA. Hydrobiologia 83:303–312.

Hall, R. O., and J. L. Tank. 2003. Ecosystem metabolism controls nitrogen uptake in streams in Grand Teton National Park, Wyoming. Limnology and Oceanography 48:1120–1128.

Hall, R. O., Jr., et al. 2009. Nitrate removal in stream ecosystems measured by ^{15}N addition experiments: total uptake. Limnology and Oceanography 54:653–665.

Hall, S. R. 2004. Stochiometrically-explicit competition between grazers: species replacement, coexistence and priority effects along resource supply gradients. American Naturalist 164:157–172.

Hall, S. R., V. H. Smith, D. A. Lytle, and M. A. Leibold. 2005. Constraints on primary producer N:P stoichiometry along N:P supply ratio gradients. Ecology 86:1894–1904.

Harrison, J. A., P. A. Matson, and S. E. Fendorf. 2005. Effects of a diel oxygen cycle on nitrogen transformations and greenhouse gas emissions in a eutrophied subtropical stream. Aquatic Sciences 67:308–315.

Hatch, L. K., J. E. Reuter, and C. R. Goldman. 1999. Daily phosphorus variation in a mountain stream. Water Resources Research 35:3783–3791.

Healey, F. P. 1973. Inorganic nutrient uptake and deficiency in algae. Critical Reviews in Microbiology 3:69–113.

Heffernan, J. B., and M. J. Cohen. 2010. Direct and indirect coupling of primary production and diel nitrate dynamics in a subtropical spring-fed river. Limnology and Oceanography 55:677–688.

Heffernan, J. B., M. J. Cohen, T. K. Frazer, R. G. Thomas, T. J. Rayfield, J. Gulley, J. B. Martin, J. J. Delfino, and W. D. Graham. 2010*a*. Hydrologic and biotic influences on nitrate removal in a sub-tropical spring-fed river. Limnology and Oceanography 55:249–263.

Heffernan, J. B., D. M. Liebowitz, T. K. Frazer, J. M. Evans, and M. J. Cohen. 2010*b*. Algal blooms and the nitrogen-enrichment hypothesis in Florida springs: evidence, alternatives, and adaptive management. Ecological Applications 20:816–829.

Hensley, R. T., and M. J. Cohen. 2012. Controls on solute transport in large spring-fed karst rivers. Limnology and Oceanography 57:912–924.

Hill, W. R., P. J. Mulholland, and E. R. Marzolf. 2001. Stream ecosystem responses to forest leaf emergence in spring. Ecology 82:2306–2319.

Hoellein, T. J., J. L. Tank, E. J. Rosi-Marshall, S. A. Entrekin, and G. A. Lamberti. 2007. Controls on spatial and temporal variation of nutrient uptake in three Michigan headwater streams. Limnology and Oceanography 52:1964–1977.

Holloway, J. M., and R. A. Dahlgren. 2001. Season and event-scale variations in solute chemistry for four Sierra Nevada catchments. Journal of Hydrology 250:106–121.

House, L. J., and W. A. House. 2002. Precipitation of calcite in the presence of inorganic phosphate. Colloids and Surfaces A: Physicochemical and Engineering Aspects 203:143–153.

House, W. A. 1990. The prediction of phosphate coprecipitation with calcite in freshwaters. Water Research 24:1017–1023.

Jarvie, H. P., C. Neal, R. J. Williams, M. Neal, H. D. Wickham, L. K. Hill, A. J. Wade, A. Warwick, and J. White. 2002. Phosphorus sources, speciation and dynamics in the lowland eutrophic River Kennet, UK. Science of the Total Environment 282–283:175–203.

Kalita, T. L., T. V. Titlyanova, and E. A. Titlyanov. 2007. New rhythmic changes in mitosis and growth in low differentiated green and red marine macroalgae. Russian Journal of Marine Biology 33:207–212.

Kerkhoff, A. J., B. J. Enquist, J. J. Elser, and W. F. Fagan. 2005. Plant allometry, stoichiometry and the temperature-dependence of primary productivity. Global Ecology and Biogeography 14:585–598.

Khailov, K. M., and Z. P. Burlakova. 1969. Release of dissolved organic matter by marine seaweeds and distribution of their total organic production to inshore communities. Limnology and Oceanography 14:521–527.

Khoshmanesh, A., B. T. Hart, A. Duncan, and R. Beckett. 2002. Luxury uptake of phosphorus by sediment bacteria. Water Research 36:774–778.

Kim, L. H., E. Choi, and M. K. Stenstrom. 2003. Sediment characteristics, phosphorus types and phosphorus release rates between river and lake sediments. Chemosphere 50:53–61.

Kimura, T., M. Watanabe, K. Kohata, and R. Sudo. 1999. Phosphate metabolism during diel vertical migration in the rephidoceaen alga *Chattonella antiqua*. Journal of Applied Phycology 11:301–311.

Kirchner, J. W., X. H. Feng, C. Neal, and A. J. Robson. 2004. The fine structure of water-quality dynamics: the (high-frequency) wave of the future. Hydrological Processes 18:1353–1359.

Klausmeier, C. A., E. Litchman, T. Daufresne, and S. A. Levin. 2004. Optimal nitrogen-to-phosphorus stoichiometry of phytoplankton. Nature 429:171–174.

Kleeburg, A., and G. Schlungbaum. 1993. In situ phosphorus release experiments in the Warnow River (Mecklenburg, northern Germany). Hydrobiologia 253:263–274.

Kuo, S. 1996. Phosphorus. Pages 869–919 *in* J. M. Bigham, editor. Methods of soil analysis, part 3: chemical methods. Soil Science Society of America, ASA, Madison, Wisconsin, USA.

Kurz, R. C., D. Woithe, S. K. Notestein, T. K. Frazer, J. A. Hale, and S. R. Keller. 2004. Mapping and monitoring submerged aquatic vegetation in Ichetucknee springs. Contract No. 02/03-180. Suwanee River Water Management District, Live Oak, Florida, USA.

Kuwabara, J. S. 1992. Associations between benthic flora and diel changes in dissolved arsenic, phosphorus, and related physicochemical parameters. Journal of the North American Benthological Society 11:218–228.

Larsson, U., and A. Hagstrom. 1979. Phytoplankton exudate release as an energy source for the growth of pelagic bacteria. Marine Biology 52:199–206.

Laursen, A. E., and S. P. Seitzinger. 2004. Diurnal patterns of denitrification, oxygen consumption and nitrous oxide production in rivers measured at the whole-reach scale. Freshwater Biology 49:1448–1458.

Lepp, P. W., and T. M. Schmidt. 1998. Nucleic acid content of *Synechococcus* spp. during growth in continuous light and light/dark cycles. Archives of Microbiology 170:201–207.

Liu, Z., X. Liu, and C. Liao. 2008. Daytime deposition and nighttime dissolution of calcium carbonate by submerged plants in a karst spring-fed pool: insights from high time-resolution monitoring of physico-chemistry of water. Environmental Geology 55:1159–1168.

Makino, W., J. B. Cotner, R. W. Sterner, and J. J. Elser. 2003. Are bacteria more like plants or animals? Growth rate and resource dependence of bacterial C:N:P stoichiometry. Functional Ecology 17:121–130.

Martin, J. B., and S. L. Gordon. 2000. Surface and ground water mixing, flow paths, and temporal variations in chemical compositions of karst springs. Pages 65–92 *in* I. E. Sasowsky and C. Wicks, editors. Groundwater flow and contaminant transport in karst aquifers. A.A. Balkema, Rotterdam, The Netherlands.

Matheson, F. E., J. M. Quinn, and M. L. Martin. 2012. Effects of irradiance on diel and seasonal patterns of nutrient uptake by stream periphyton. Freshwater Biology 57:1617–1630.

McKnight, D., and K. E. Bencala. 1988. Diel variations in iron chemistry in an acidic stream in the Colorado Rocky Mountains, USA. Arctic and Alpine Research 20:492–500.

Meyer, J. L., and G. E. Likens. 1979. Transport and transformation of phosphorus in a forest stream ecosystem. Ecology 60:1255–1269.

Mulholland, P. J., et al. 2008. Stream denitrification across biomes and its response to anthropogenic nitrate loading. Nature 452:202–205.

Mulholland, P. J., E. R. Marzolf, J. R. Webster, D. R. Hart, and S. P. Hendricks. 1997. Evidence that hyporheic zones increase heterotrophic metabolism and phosphorus uptake in forest streams. Limnology and Oceanography 42:443–451.

Newbold, J. D., J. W. Elwodd, R. V. O'Neill and A. L. Sheldon. 1983. Phosphorus dynamics in a woodland stream ecosystem: a study of nutrient spiraling. Ecology 64:1249–1265.

Newbold, J. D., J. W. Elwood, R. V. O'Neill, and W. van Winkle. 1981. Measuring nutrient spiraling in streams.

Canadian Journal of Fisheries and Aquatic Sciences 38:860–863.

Nimick, D. A., C. H. Gammons, and S. R. Parker. 2011. Diel biogeochemical processes and their effect on the aqueous chemistry of streams: A review. Chemical Geology 283:3–17.

Odum, H. T. 1956. Primary production in flowing waters. Limnology and Oceanography 1:102–117.

Odum, H. T. 1957. Primary production measurements in eleven Florida springs and a marine turtle-grass community. Limnology and Oceanography 1:85–97.

Owens, M. 1974. Measurements on non-isolated natural communities in running waters. Pages 111–119 *in* R. A. Vollenweider, editor. A manual on methods for measuring primary production in aquatic environments. Blackwell Scientific Publications, Oxford, UK.

Parker, S. R., C. H. Gammons, S. R. Poulson, and M. D. DeGrandpre. 2007. Diel variations in stream chemistry and isotopic composition of dissolved inorganic carbon, upper Clark Fork River, Montana, USA. Applied Geochemistry 22:1329–1343.

Passow, U. 2002. Transparent exopolymer particles (TEP) in aquatic environments. Progress in Oceanography 55:287–333.

Pellerin, B. A., B. D. Downing, C. Kendall, R. A. Dahlgren, T. E. C. Krauss, J. F. Saraceno, R. G. M. Spencer, and B. A. Bergamaschi. 2009. Assessing the sources and magnitude of diurnal nitrage variability in the San Joaquin River (California) with an in situ optical nitrate sensor and dual nitrate isotopes. Freshwater Biology 54:376–387.

Pellerin, B. A., J. F. Saraceno, J. B. Shanley, S. D. Sebestyen, G. R. Aiken, W. M. Wollheim, and B. A. Bergamaschi. 2012. Taking the pulse of snowmelt: in situ sensors reveal seasonal, event and diurnal patterns of nitrate and dissolved organic matter variability in an upland forest stream. Biogeochemistry 108:183–198.

Persson, J., P. Fink, A. Goto, J. M. Hood, J. Jonas, and S. Kato. 2010. To be or not to be what you eat: regulation of stoichiometric homeostasis among autotrophs and heterotrophs. Oikos 119:741–751.

Plant, L. J., and W. A. House. 2002. Precipitation of calcite in the presence of inorganic phosphate. Colloids and Surfaces A: Physicochemical and Engineering Aspects 203:143–153.

Reddy, K. R., R. H. Kadlec, E. Falig, and P. M. Gale. 1999. Phosphorus retention in streams and wetlands: a review. Critical Reviews in Environmental Science and Technology 29:83–146.

Roberts, B. J., and P. J. Mulholland. 2007. In-stream biotic control on nutrient biogeochemistry in a forested stream, West Fork of Walker Branch. Journal of Geophysical Research 112:G04002.

Roberts, B. J., P. J. Mulholland, and W. R. Hill. 2007. Multiple scales of temporal variability in ecosystem metabolism rates: results from 2 years of continuous monitoring in a forested headwater stream. Ecosystems 10:588–606.

Rusjan, S., and M. Mikos. 2010. Seasonal variability or diurnal in-stream nitrate concentration oscillations under hydrologically stable conditions. Biogeochemistry 97:123–140.

Schade, J. D., J. F. Espeleta, C. A. Klausmeier, M. E. McGroddy, S. A. Thomas, and L. X. Zhang. 2005. A conceptual framework for ecosystem stoichiometry: Balancing resource supply and demand. Oikos 109:40–51.

Schade, J. D., K. MacNeill, S. A. Thomas, F. C. McNeely, J. R. Welter, J. Hood, M. Goodrich, M. E. Power, and J. C. Finlay. 2011. The stoichiometry of nitrogen and phosphorus spiralling in heterotrophic and autotrophic streams. Freshwater Biology 56:424–436.

Schindler, D. W. 1977. Evolution of phosphorus limitation in lakes. Science 195:260–262.

Simal, J., M. Lage, and I. Iglesias. 1985. Second derivative UV spectroscopy and sulfamic acid method for determination of nitrate in water. Journal of Analytical Chemistry 68:962–964.

Smith, V. H. 2003. Eutrophication of freshwater and coastal marine ecosystems—a global problem. Environmental Science and Pollution Research 10:126–139.

Sterner, R. W., and J. J. Elser. 2002. Ecological stoichiometry: the biology of elements from molecules to the biosphere. Princeton University Press, Princeton, New Jersey, USA.

Tank, J. L., E. J. Rosi-Marshall, M. A. Baker, and R. O. Hall, Jr. 2008. Are rivers just big streams? A pulse method to quantify nitrogen demand in a large river. Ecology 89:2935–2945.

Tate, C. M., R. E. Broshears, and D. M. McKnight. 1995. Phosphate dynamics in an acidic mountain stream: interactions involving algal uptake, sorption by iron oxide and photoreduction. Limnology and Oceanography 40:938–946.

Triska, F. J., V. C. Kennedy, R. J. Avanzino, G. W. Zellweger, and K. E. Bencala. 1989. Retention and transport of nutrients in a third-order stream: channel processes. Ecology 70:1877–1892.

Vincent, W. F., and M. T. Downes. 1980. Variation in nutrient removal from a stream by watercess (*Nasturtium officinale* R. Br.). Aquatic Botany 9:221–235.

Vitousek, P. M. 1982. Nutrient cycling and nutrient use efficiency. American Naturalist 119:553–572.

Vrede, T., D. R. Dobberfuhl, S. Kooijman, and J. J. Elser. 2004. Fundamental connections among organism C:N:P stoichiometry, macromolecular composition, and growth. Ecology 85:1217–1229.

Webster, I. T., N. Rea, A. V. Padovan, P. Dostine, S. A. Townsend, and S. Cook. 2005. An analysis of primary production in the Daly River, a relatively unimpacted tropical river in northern Australia. Marine and Freshwater Research 56:303–316.

Wollheim, W. M., C. J. Voosmarty, B. J. Peterson, S. P. Seitzinger, and C. S. Hopkinson. 2006. Relationship between river size and nutrient removal. Geophysical Research Letters 33. http://dx.doi.org/10.1029/2006GL025845

Zarnetske, J. P., R. Haggerty, S. M. Wondzell, and M. A. Baker. 2011. Labile dissolved organic carbon supply limits hyporheic denitrification. Journal of Geophysical Research 116:G04036.

Supplemental Material

Appendix A

Map of the study site (*Ecological Archives* M083-007-A1).

Appendix B

Images of the Ichetucknee River (*Ecological Archives* M083-007-A2).

Supplement

Data files to calculate nutrient removal and daily metabolism, summary of autotroph tissue stoichiometry, and proxy estimation of diel calcium variation (*Ecological Archives* M083-007-S1).